AD-A182 571 THRUST CONTROL WITH HIGH PRESSURE RATIO EJECTOR AUGMENTORS(U) AERONAUTICAL RESEARCH LABS MELBOURNE (AUSTRALIA) S C FAVALORO AUG 86 ARL/AERO/PROP-R-173 1/1

UNCLASSIFIED F/G 21/2 NL

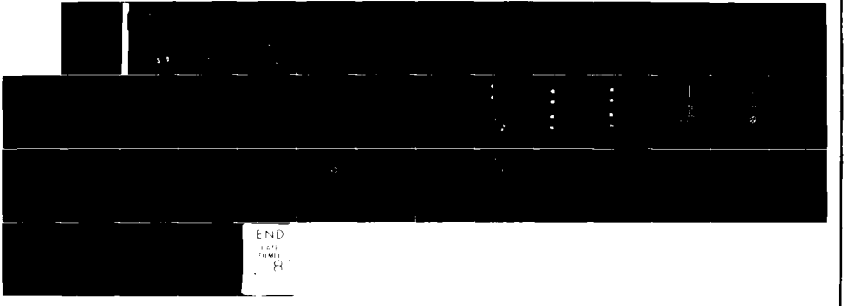

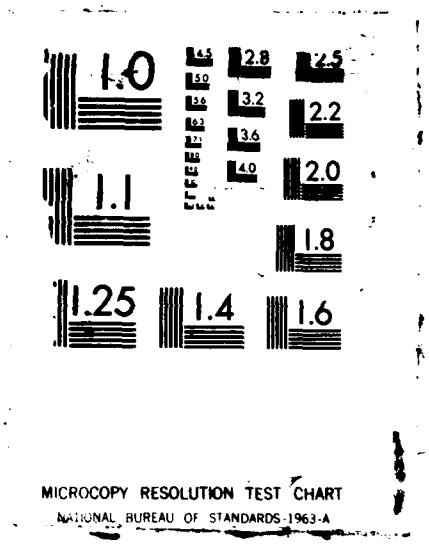
1.0
1.1
1.25
1.4
1.6
1.8
2.0
2.2
2.5
2.8
3.2
3.6
4.0
4.5
5.0
5.6
6.3
7.1
8.0
MICROCOPY RESOLUTION TEST CHART
NATIONAL BUREAU OF STANDARDS-1963-A

ARL-AERO PROP R-173 AR-004-500

DEPARTMENT OF DEFENCE

DEFENCE SCIENCE AND TECHNOLOGY ORGANISATION

AERONAUTICAL RESEARCH LABORATORIES

MELBOURNE, VICTORIA

Aero Propulsion Report 173

THRUST CONTROL WITH HIGH PRESSURE RATIO EJECTOR AUGMENTORS

by

S.C.FAVALORO

Approved for Public Release

August 1986

AR-004-500

DEPARTMENT OF DEFENCE
DEFENCE SCIENCE AND TECHNOLOGY ORGANISATION
AERONAUTICAL RESEARCH LABORATORIES

Aero Propulsion Report 173

THRUST CONTROL WITH HIGH PRESSURE RATIO EJECTOR AUGMENTORS

by

S.C. FAVALORO

SUMMARY

The possibility of utilising the entrained secondary air in a thrust augmenting ejector for thrust control purposes has been examined in a series of experiments using high pressure unheated air as the primary jet.

Four control concepts, namely duct venting, axially deployed spoilers, radially deployed tabs and duct swivelling, have been investigated and results have shown that all systems provide some degree of thrust vector and thrust magnitude control. Maximum TVC in yaw/pitch mode was available with duct swivelling, while radial tabs provided maximum TMC.

POSTAL ADDRESS: Director, Aeronautical Research Laboratories,
P.O. Box 4331, Melbourne, Victoria, 3001, Australia.

CONTENTS

NOMENCLATURE

$A_{v,s,t}$	-	control element surface areas
$C_{x,y,x}$	-	moments about axes
D	-	diameter of parallel mixing section
F_n	-	theoretical ejector force components
L	-	length of parallel mixing section
M	-	Mach number
P_a	-	atmospheric pressure
P_{ot}	-	primary nozzle total pressure
S	-	ejector side force
T_E	-	ejector thrust
T_P	-	primary nozzle thrust
α	-	ejector swivel angle
θ	-	angle to ejector axis
κ	-	area ratio
τ	-	thrust augmentation ration = $\frac{T_P + T_E}{T_P}$

Subscripts

n	-	variable, relating to force number
s	-	relating to spoiler
t	-	relating to tab
v	-	relating to vent
x,y,z	-	relating to orthogonal axes

Abbreviations

COG	-	centre of gravity
NEP	-	primary nozzle exit plane
TMC	-	thrust magnitude control
TVC	-	thrust vector control

1. INTRODUCTION

There are a number of possible systems for thrust vector control (TVC) and thrust magnitude control (TMC) for rocket powered vehicles, the complexity of which vary according to the degree of control required. The most complex systems generate roll, pitch and yaw moments as well as axial thrust control, all of which can be varied in magnitude during flight, while simpler systems provide for only one or two control moments which are fixed in magnitude.

Conventional systems operate by the reaction to gas loads on control elements deployed asymmetrically in the rocket exhaust for TVC, or symmetrically for TMC. Typical elements include tabs or vanes deployed from the sides of the vehicle, and airfoil sections which are permanently stationed in the exhaust gas. However, the availability of materials capable of withstanding the high stagnation temperatures and pressures in a rocket efflux during sustained flight can be a significant problem. Other thrust control systems under investigation, such as off-axis propellant burning and boundary layer control in overexpanded nozzles alleviate the material problem, but can introduce complexities of their own.

One application which requires sophisticated control is the hovering rocket, and a tab/vane system providing full TVC and TMC has been developed for that purpose [1]. The addition of a thrust augmenting ejector duct to the rocket vehicle would improve the thrust efficiency at hover and low speed conditions, but would almost certainly be incompatible with the tab/vane control system acting directly in the rocket efflux, due to deflected hot gases impinging on the ejector body, and the possibility of afterburning of the fuel rich exhaust in the duct. However, there is possible advantage in the availability of the cooler entrained airstream for control purposes, which would completely eliminate the material problem.

As part of a general study of high pressure ratio ejector augmentors for use with hovering rockets ([2], [3], [4], [5]) this report examines several TVC and TMC systems suitable for thrust augmented jets.

2. EJECTOR PERFORMANCE

2.1. General

A rocket motor is particularly inefficient at static or low speed conditions, due to the poor propulsive efficiency of the high velocity jet. This efficiency can be improved by the addition of a non-afterburning thrust augmenting ejector (Figure 1), in which part of the energy in the high velocity jet is used to entrain atmospheric air to increase the mass flow and reduce the velocity in the final jet. The ejector is most effective at low speeds, where the gain in propulsive efficiency is maximised and is not outweighed by the momentum drag of the induced flow and the aerodynamic drag on the ejector body. The static performance of axisymmetric ejectors with both high pressure air jets and rocket motors has been explored at ARL and WSRL ([2], [3], [4], [5]) and useful levels of thrust augmentation have been demonstrated.

Thrust control systems operating in the entrained airflow will be most effective when the mass flow of the entrained air is maximised. The level of entrainment, for a given mixing duct diameter, depends primarily upon the completeness of mixing between the two flows in the ejector - increasing the ejector length or using enhanced mixing devices, such as a nozzle with multiple lobes at its exit plane, optimise the mixing process. It should be noted that in the test series described in this paper, no diffuser was added and complete mixing of the two flows at the ejector exit plane was not possible, due to constraints imposed on the geometric configuration of the test model [2].

2.2. Ejector Forces

As the entrained air is accelerated into the ejector, suction pressures develop across the inlet and along the walls of the mixing duct. These are illustrated schematically in Figure 2 which shows a sectioned view of a parallel sided ejector with a qualitative indication of the pressure distribution and resultant force components (Figure 2(a)), and a perspective view showing the sign convention adopted for side (radial) forces and moments at the nozzle exit plane (Figure 2(b)). It is apparent

that a measure of thrust control can be achieved by manipulating the magnitude or line of action of the resultant forces. Moment vectors of varying magnitude will be generated in the x-y plane if the distribution of axial force components on the bellmouth is changed asymmetrically, or if the magnitude or line of action of the radial forces are altered; thrust magnitude control only will be available if the force manipulations are symmetric.

The amount of control which can be achieved using forces associated with the entrained flow is related to the initial level of thrust augmentation, τ. The maximum TMC capability is in the order of τ-1 (ie 100% of ejector thrust is spoiled). Peak performance in TVC depends on the magnitude and line of action of the resultant side (radial) force, and the moment available at the nozzle exit plane (NEP) due to asymmetry in axial force components.

3. THRUST CONTROL SYSTEMS

Four potential thrust control systems, namely duct venting, axial and radially deployed tabs, and duct swivelling were investigated in the test series. The systems aimed to provide moments (pitch and yaw only - no spin moment) about a host vehicle COG, and axial thrust control by acting in and on the entrained air, without interfering with the primary jet flow.

3.1. Atmospheric Venting

If a vent is introduced in the ejector wall downstream of the NEP, the pressure distribution should qualitatively resemble that shown in Figure 3(a). Changes in the magnitude and line of action of the force acting on the section of the inlet adjacent to the vent (F_2 and θ_v, cf F_1 and θ), as well as changes in the radial force distribution on the ejector wall, should result in a net moment and side force at the NEP, with some reduction in axial thrust. TMC with no TVC could be achieved with symmetrical venting around the duct periphery.

3.2. Tab (spoilers) - Axial Deployment

In a similar fashion, axial deployment of a spoiler (tab) past the NEP will disrupt the entrainment process to give a force distribution which may resemble that shown in Figure 3(b). Depending on the relative magnitudes and lines of action of the forces acting on different sections of the augmentor, it is apparent that a moment and a thrust reduction would eventuate. As before, TMC alone will be realised if a number of spoilers, distributed symmetrically around the inlet, are evenly deployed.

3.3. Tabs - Radial Deployment

A tab deployed radially into the entrained airstream within the ejector duct, at some distance downstream of the NEP, may produce a pressure distribution similar to that shown in Figure 3(c). Once again, resultant forces on the inlet and wall adjacent to the tab, plus the additional drag force, F_5, acting on the tab, may combine to give a moment and side force at the NEP, with some reduction in axial thrust. Equal deployment of several tabs, distributed symmetrically around the duct wall, should give TMC only.

3.4. Ejector Duct Swivelling

Rotation of the ejector body about the NEP (Figure 3(d)) changes the line of thrust developed by the ejector to give a moment about a nominal vehicle COG. Depending on the degree of rotation, α , the pressure distribution may not be symmetrical about the ejector axis; hence, a moment and side force at the NEP may also be generated. When the line of action of the ejector thrust changes, some loss in axial thrust can be expected. TMC alone, for the duct swivel system, would be achieved either in combination with one of the other systems, or by axial translation of the ejector body. Axial translation was not a subject of the present tests.

4. EXPERIMENT

4.1. Rig

Figure 4 shows a schematic illustration of the test rig. The primary air comes from storage vessels at a pressure of 7 MPa and at room temperature. The air is regulated to the required test pressure and expanded in a convergent-divergent nozzle to form the high velocity jet. The test nozzle has an expansion ration of 4.03, and is shaped internally to provide a smooth transition from a circular throat to a three lobe cross section (Figure 4) at the exit plane. Primary nozzle thrust is measured by a force transducer as shown in Figure 4.

The axisymmetric ejector model consists of a bellmouth inlet and a parallel mixing tube of length L and internal diameter D. Each thrust control system (except Duct Swivelling) consists of three control elements which are mounted symmetrically (120° spacing) around the periphery of a sleeve, diameter D, and located in the mixing tube as shown in Figure 4. The overall L/D ratio of the ejector/control system combination is approximately 5, while the ejector inlet area/nozzle exit area ratio is nominally 36.

The ejector is mounted horizontally on a three component force table, with provision for rotation of the duct about the vertical axis. The table consists of two rigid aluminium plates connected to each other and to ground by supports which flex in one plane only. Axial forces are transmitted to the upper plate only and measured by a single force transducer, while side forces and moments acting on the ejector are transmitted to the lower plate and measured by two force transducers.

4.2. Instrumentation

Calibration and test data from the transducers were processed on a Hewlett Packard 3052A Data Acquisition System (DAS). The calibration and data reduction methods are described in detail in the Appendix.

4.3. Method

The characteristics of the control devices were investigated by progressive deployment of the control elements, either symmetrically for TMC or asymmetrically for TVC, as shown in Figure 5. A single element was deployed in the TVC tests and the ejector model was aligned so that the side force and moment on the ejector were at a maximum in the plane of the two transversely orientated transducers. TVC tests with duct swivelling were performed by rotating the duct up to 5° about the NEP at invervals of 1°.

Tests were performed with two nozzle orientations, namely;

(i) with each nozzle lobe adjacent to a control element, and

(ii) each nozzle lobe midway between two elements - i.e. the nozzle was rotated through 60° (Figure 5).

Tests were also performed at two primary blowing pressures, namely 3.4 MPa, where the flow was correctly expanded by the nozzle, and at 4.2 MPa, where the flow was underexpanded.

5. RESULTS AND DISCUSSION

The results from the TMC experiments are presented as plots of thrust augmentation ratio, τ, against a parameter, κ, which represents the degree of interference each control system imposes on the entrained airstream, and is defined as:

$$\kappa = \frac{A_{v,s,t}}{D^2/4} \times 100, \text{ where}$$

A_v = area of vent(s) opening,

A_s = area of spoiler(s) deployed past the NEP,

A_t = area of tab(s), normal to the ejector axis.

Figure 6 shows how κ varies with component deployment for both TMC and TVC.

The TVC results are presented in terms of side force/primary thrust, NEP moments and ejector inlet Mach number distributions plotted against the area ratio, κ.

5.1. Duct Venting

5.1.1. TMC

The performance of the circumferential vents in TMC is shown in Figure 7. A spoilage of approximately 9% of total augmented thrust (~ 30% of ejector thrust) was available with the primary jet correctly expanded and all vents fully open. Marginally lower spoilage levels resulted with the underexpanded jet, and with the nozzle lobes midway between the vents. To achieve control to 100% of ejector thrust, it is apparent that the vent area would need to be increased substantially.

5.1.2. TVC

Figure 8 shows the side force and moment obtained from asymmetric duct venting. Up to the limit of open area available with a single vent, both the side force and moment were small, with the experimental scatter being of similar order to the mean quantities. A reason for the lack of significant moments is seen in Figure 9, which shows a plot of Mach number distribution around the internal bellmouth periphery against the area ratio. The degree of venting available clearly failed to produce the level of asymmetry in the ejector inlet flow required for significant lateral forces and moments. Positioning of the vents further upstream, greater vent open area, or probably both, would be required to increase the system control capability.

5.2. Axial Spoilers

5.2.1. TMC

Figure 10 shows the results from symmetric deployment of the axial spoilers. A reduction of approximately 13% of total augmented thrust (~ 45% of ejector thrust) was achieved with the spoilers fully

deployed, and with the nozzle in either orientation. As with the vents, a more substantial spoilage would result if the spoiler area was increased.

5.2.2. TVC

Figure 11 shows the results of asymmetric spoiler deployment. Side forces were small (<1% of primary thrust), but there were significant negative moments available with both nozzle orientations at both test pressures.

In terms of the model developed earlier (Figure 3(b)), negative moments about the NEP will be produced if the couple due to F_2 and F_4 is greater than the couple due to F_1 and F_3. This can occur if there are changes in either the magnitude or line of action (or both) of F_2 and F_3 - evidence of a positive resultant side force suggests a change in the line of action. The larger moment generated with a nozzle lobe adjacent to the spoiler indicates that the line of action of F_2 and F_3 moved further upstream, relative to the other nozzle orientation.

The effect of a further increase in spoiler area on the system performance in TVC is difficult to predict. The trends of side force and NEP moment in Figure 11 suggest that with such an increase, the moment about a nominal vehicle COG would be reduced, since the moment due to the side force and the NEP moment began to oppose each other at higher levels of spoiler deployment.

Plots of surface Mach number around the inlet (Figure 12) show that there was little change in the inlet pressure distribution from the unvectored configuration in areas remote from the deployed spoiler (pressure tappings 3 and 4). However, complete information about the level of asymmetry in the inlet pressure distribution was unavailable, since the deployed spoiler completely covered tapping 1, and the leading edge of another spoiler interfered with tapping 2.

5.3. Radial Tabs

5.3.1. TMC

Figure 13 shows the performance of symmetrically deployed radial tabs in TMC. A spoilage of approximately 30% of total augmented thrust (100% ejector thrust) was achieved with only 50% (κ = 25%) deployment of the tabs. Further deployment resulted in exceptionally large spoilage levels - up to 85% of total augmented thrust.

Differences due to nozzle orientation were first detected at 75% (κ = 40%) deployment - with the nozzle in the 0° configuration, the radially disposed sheets of the primary jet had evidently began to impinge upon the tabs, promoting a larger spoilage than the alternate nozzle configuration.

This situation would be undesirable in practice, and inconsistent with the aim of operating the control devices in the cooler entrained airstream only.

5.3.2. TVC

Results from asymmetric tab deployment (Figure 14) presented a more complex picture - small positive side forces and moments were generated with the deployed tab adjacent to a nozzle lobe, while predominantly negative side forces and moments were generated with the alternate configuration.

Mach number plots around the inlet (Figure 15) showed that the entire force distribution on the inlet was affected, although the maximum effect was on the section of the inlet adjacent to the deployed tab (tapping 1).

Since there was no significant change in the inlet Mach number distribution for the alternate nozzle orientation (the results are omitted from Figure 15 for clarity), the reasons for the difference in side force and moment between the two configurations appear to lie in the force distribution on the parallel mixing section of the ejector.

It can be argued that drag forces on the tab (F_5, Figure 4(c)) are greater with the tab adjacent to a nozzle lobe, and hence promote positive (clockwise) moments at the NEP. But the pattern of side force and moment (Figure 14) suggests that the side forces are the principal generators of the moment, indicating substantial differences due to nozzle orientation in the lines of action and/or magnitudes of F_{31}, F_{32} & F_4 (Figure 3(c)). The reason for the different results between nozzle orientations is not immediately apparent. More detailed measurements of the ejector forces would be required to resolve the problem.

5.4. Comparisons

A comparison of the first three systems in TMC is shown in Figure 16. It was evident that for a given effective area ratio, κ, radially deployed control elements achieved a higher thrust spoilage than either venting or axially deployed systems.

Figure 17 shows plots of moments about a notional vehicle COG, centred one metre from the NEP, and associated thrust spoilage for deployment of a single element from each control system. The performance in TVC of each control device was comparable but, as expected, the associated thrust spoilage was larger with the radial tab.

5.5. Duct Swivelling

Substantial positive side forces and moments were generated at the NEP when the ejector was rotated 5° counter-clockwise about the NEP (Figure 18). Further duct rotation would have caused the expanded primary jet to impinge on the ejector walls at the exit plane. The existance of a moment at the NEP indicated that the pressure distribution on the ejector walls changed asymmetrically as the duct was rotated, if it is assumed that the relative lines of action of the forces on the inlet did not change. No distributions of Mach number around the inlet were available to confirm this latter assumption.

Figure 19 shows the moment at a vehicle COG, one metre from the NEP, and the thrust spoilage associated with ejector rotation. The performance is

evidently superior to the previous systems, with moments being up to an order of magnitude greater, while the thrust loss was comparable.

6. CONCLUSIONS

The possibility of using the entrained airstream in a thrust augmenting ejector for thrust control purposes was examined in a series of experiments, using high pressure unheated air to simulate a primary rocket jet. Four separate control systems, namely ejector duct venting, axially deployed spoilers, radially deployed tabs and duct swivelling, were investigated. All systems provided some degree of thrust magnitude control (TMC) and thrust vector control (TVC), but only duct swivelling in TVC (pitch/yaw mode only) and radially deployed tabs in TMC were comparable to conventional systems, in terms of the level of thrust control available.

Variation of blowing pressure, such that the primary nozzle flow ranged from correctly expanded to underexpanded, had no significant effect on the performance of the different systems, but in some cases, the orientation of the nozzle lobes, relative to the individual control elements, did have a pronounced effect.

ACKNOWLEDGEMENTS

The assistance of Mr S.A. Fisher and Dr A.M. Abdel-Fattah during many discussions, and Mr M.A. Fisher in conducting the experimental programme is gratefully acknowledged.

REFERENCES

[1] Deans, A.L. (1983). 'A Four Component Thrust Control Mechanism for a Long-Burning-Time Solid Rocket', W.S.R.L. Report WSRL-0344-TR Parts 1 & 2 (Restricted), December 1983.

[2] Fisher, S.A. (1980). 'Thrust Augmenting Ejectors for High Pressure Ratio Propulsive Jets', 7th Australasian Hydraulics and Fluid Mechanics Conference, Brisbane, August 1980.

[3] Fisher, S.A. and Irvine, R.D. (1981). 'Air Augmentation of Rockets for Low Speed Application', 5th International Symposium on Air Breathing Engines, Bangalore, February 1981.

[4] Abdel-Fattah, A.M. (1984). 'A Theoretical Study of Two Stage Thrust Augmenting Ejectors', A.R.L. Aero Propulsion Report 166, 1984.

[5] Irvine, R.D. (1983). 'Static Thrust Augmentation of Rocket Motors by Air Entrainment', WSRL Report WSRL-0332-TR, September 1983.

APPENDIX

Table 1 lists the transducers used on the rig. Data from the transducers was sent to a Hewlett Packard 3052A Data Acquisition System (DAS), comprised of a multi-channel relay scanner, a high accuracy digital voltmeter and a programmable controller/calculator, all interfaced to an IEEE bus.

TABLE 1

TRANSDUCER CHARACTERISTICS

MAKE	TYPE	MODEL	RANGE	USE
Interface	Load Cell	SM-250	0 - 250 lbf	Measure Primary Thrust
Interface	Load Cell	SM-50	0 - 50 lbf	Measure Ejector Thrust
Interface (2 off)	Load Cell	SM-10	0 - 10 lbf	Measure Ejector Side Force and Moment
Statham	Pressure Transducer		15 PSID	Measure Bellmouth Static Pressure (Connected to scanivalve)

CALIBRATION

(a) Axial Transducers

The transducers for primary and ejector thrust measurement were calibrated by attaching a series of weights to pulleys, which loaded the nozzle assembly and the ejector model independently. Calibration coefficients were calculated using a least squares method, and stored on the DAS.

(b) Side Force/moment transducers

Figure A1(a) shows a typical resultant force system for an ejector subjected to some TVC. Figure A1(b) shows the same system, resolved at the NEP. The transverse transducers (1 and 2, Figure A1) were calibrated to record the resultant moment, C, and side force, S. at the NEP as follows.

Let R_1 and R_2 equal the readings (in volts) from transducers 1 and 2 respectively. It is apparent that R_1 and R_2 depend on both S and C. Hence, equations of the form

$$R_1 = \frac{\partial R_1}{\partial S} S + \frac{\partial R_1}{\partial C} C + a_1 \qquad (1)$$

$$R_2 = \frac{\partial R_2}{\partial S} S + \frac{\partial R_2}{\partial C} + a_2 \qquad (2)$$

can be formed, where $\frac{\partial R_1}{\partial S}$, $\frac{\partial R_2}{\partial S}$, $\frac{\partial R_1}{\partial C}$ and, $\frac{\partial R_2}{\partial C}$ are calibration constants. The two remaining terms, a_1 and a_2, represent the zero offset of the transducers (i.e. under zero load). Once all of these constants are known, S and C can be computed by solving (1) and (2) simultaneously, viz:

$$C = [(R_2 - a_2) - \frac{\partial R_2}{\partial S} S] / \frac{\partial R_2}{\partial C}$$

$$S = [\frac{\partial R_2}{\partial C} (R_1 - a_1) - \frac{\partial R_1}{\partial C} (R_2 - a_2)] / [\frac{\partial R_2}{\partial C} \frac{\partial R_1}{\partial S} - \frac{\partial R_1}{\partial C} \frac{\partial R_2}{\partial S}]$$

The calibration constants were calculated by:

(1) transversely loading the ejector model along its axis of symmetry with a series of weights attached to pulleys at a number, n, of specified locations, distance z from the NEP,

(2) plotting the transducer read out, R, against applied load, for each transducer, at each location z and using a least squares routine to find n distinct calibration coefficients, ie $\frac{\partial R_1}{\partial S_i}$, $\frac{\partial R_2}{\partial S_i}$, i = 1, n

(3) plotting $\frac{\partial R_1}{\partial S_i}$, $\frac{\partial R_2}{\partial S_i}$ against the axial location z, and using a least squares routine to determine the slope and ordinate intercept of the curves for each transducer.

The slope of the curves in step (3), namely

$\frac{d}{dz}\left(\frac{\partial R_1}{\partial S_i}\right)$ and $\frac{d}{dz}\left(\frac{\partial R_2}{\partial S_i}\right)$ gave $\frac{\partial R_1}{\partial C}$ and $\frac{\partial R_2}{\partial C}$ respectively,

while the value of the ordinate at z = 0 (ie the NEP) gave $\frac{\partial R_1}{\partial S}$ and $\frac{\partial R_2}{\partial S}$.

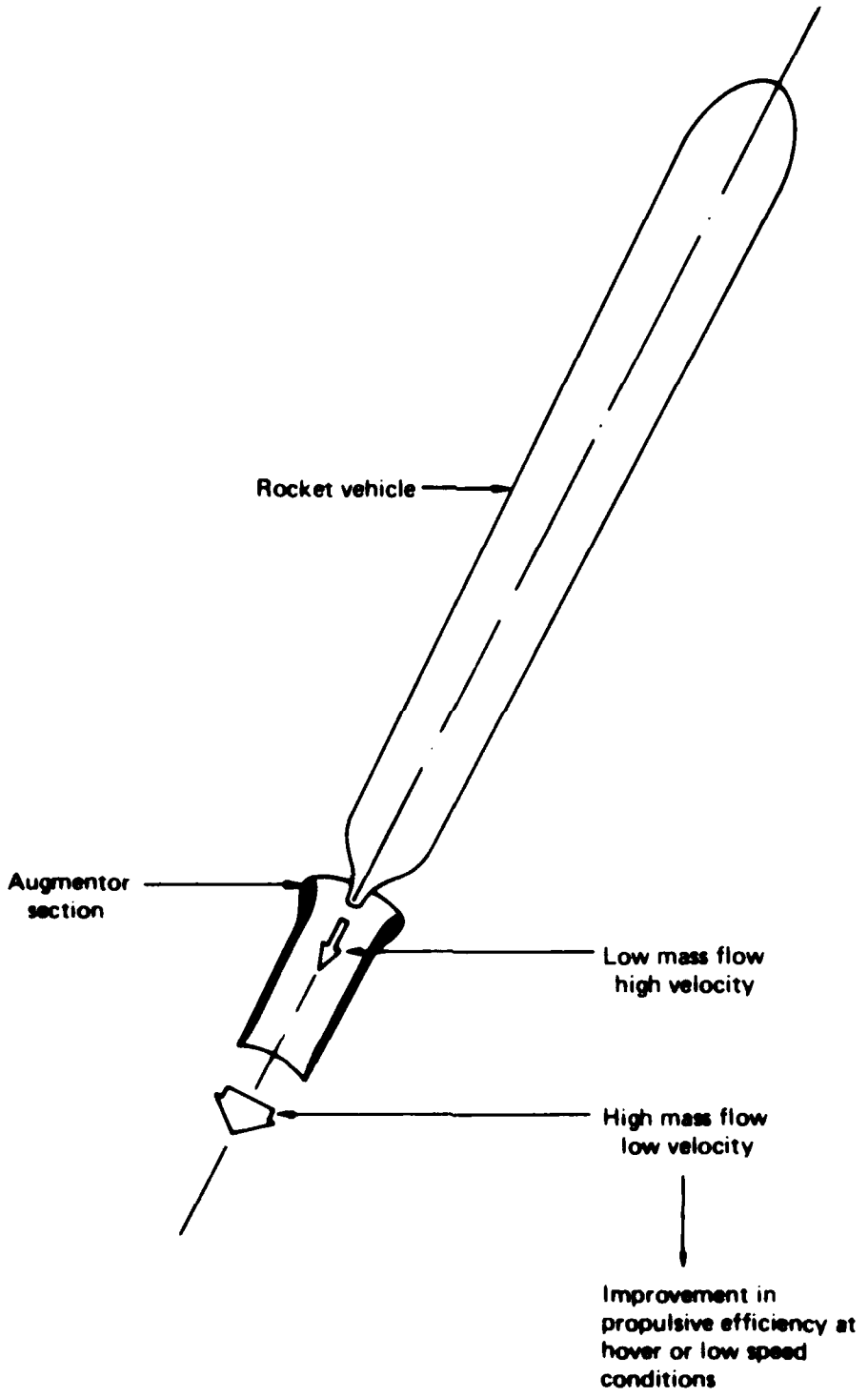

FIG. 1 APPLICATION OF EJECTOR AUGMENTOR

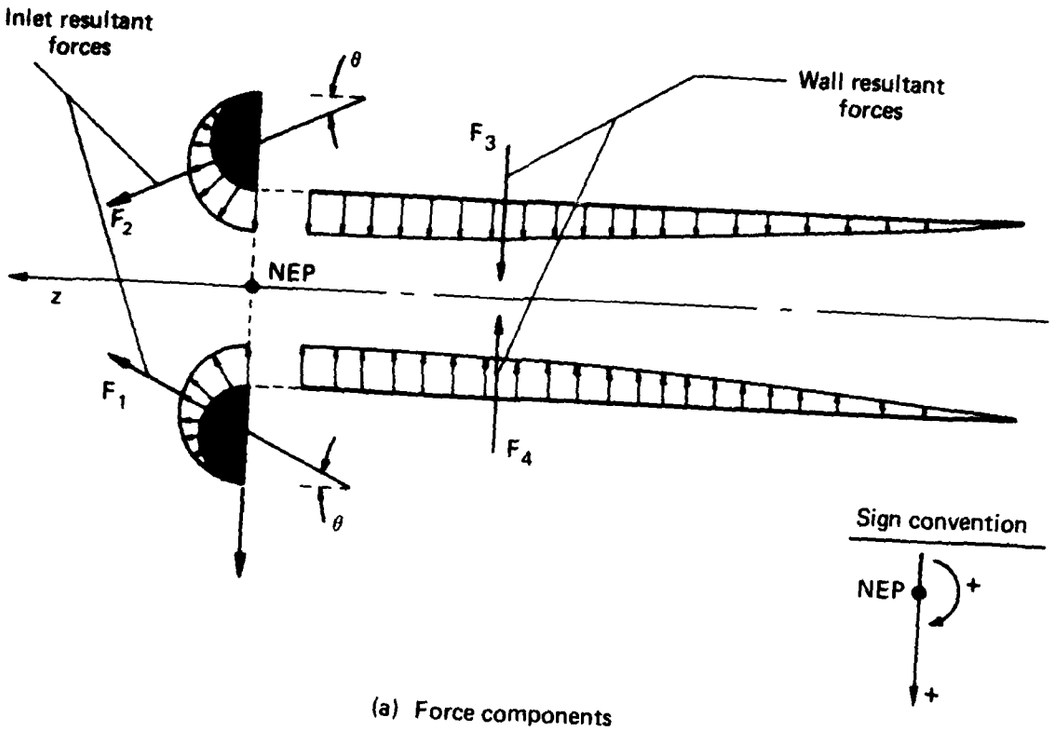

(a) Force components

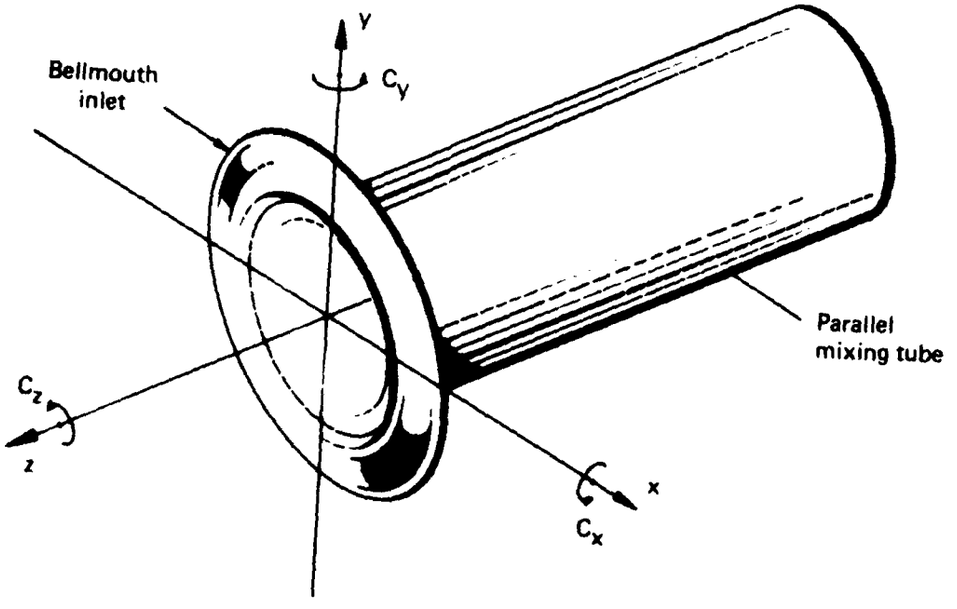

(b) Definition of axes

FIG. 2 EJECTOR FORCES & MOMENTS

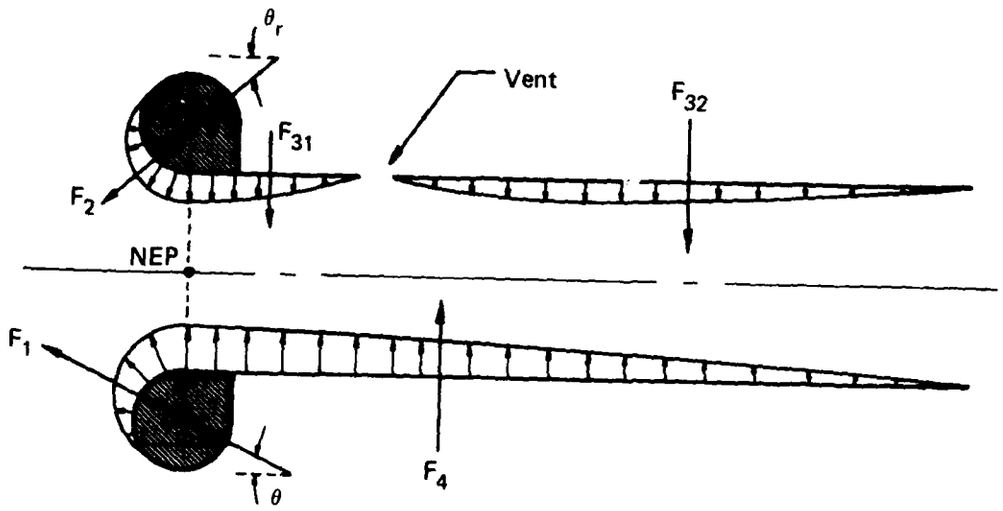

(a) Circumferential venting

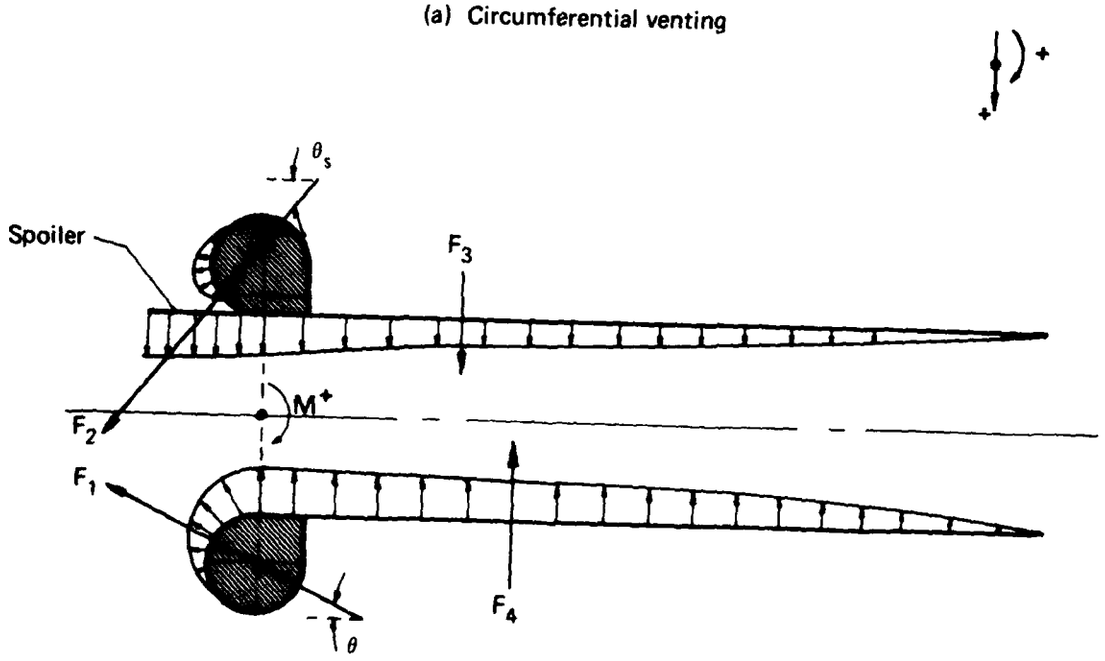

(b) Axial spoilers

FIG. 3 EJECTOR FORCE CONTROL CONERAYS

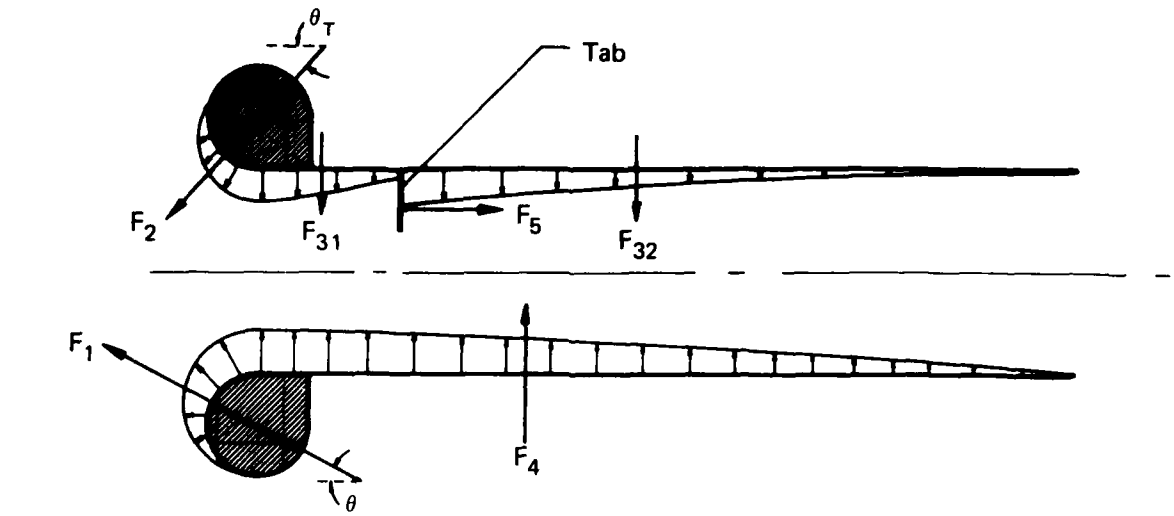

(c) Radial tab

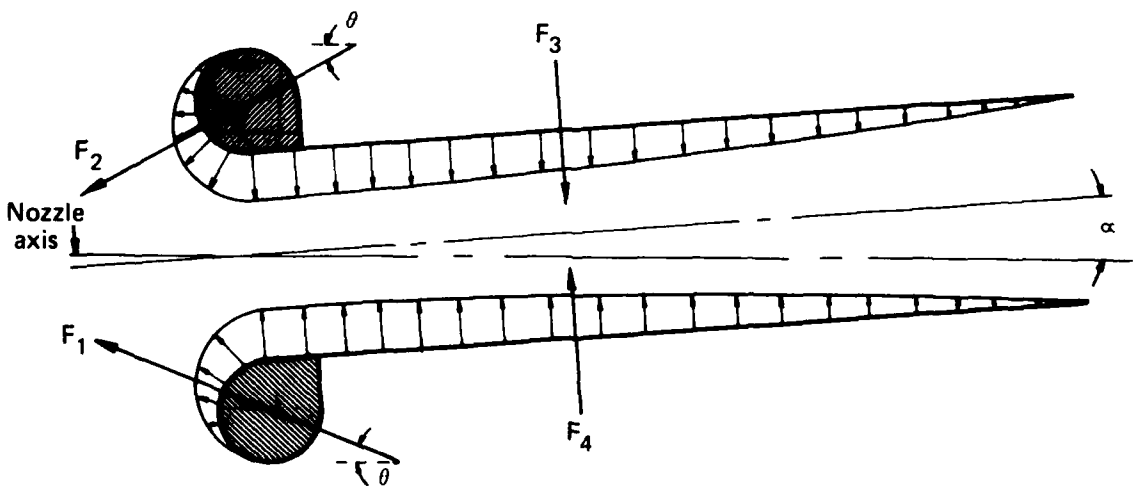

(d) Duct swivelling

FIG. 3 CONT'D

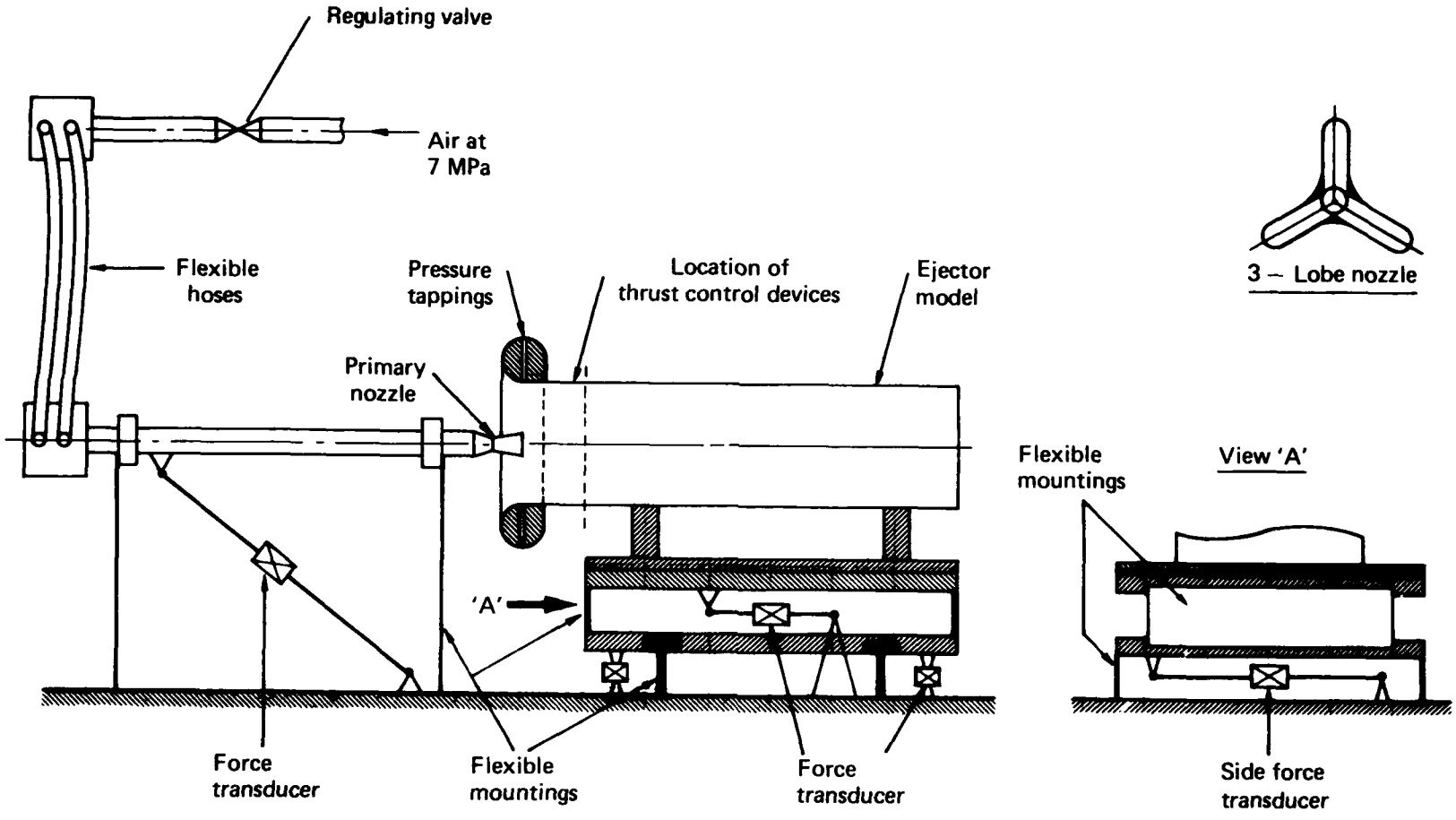

FIG. 4 EXPERIMENTAL RIG (NOT TO SCALE)

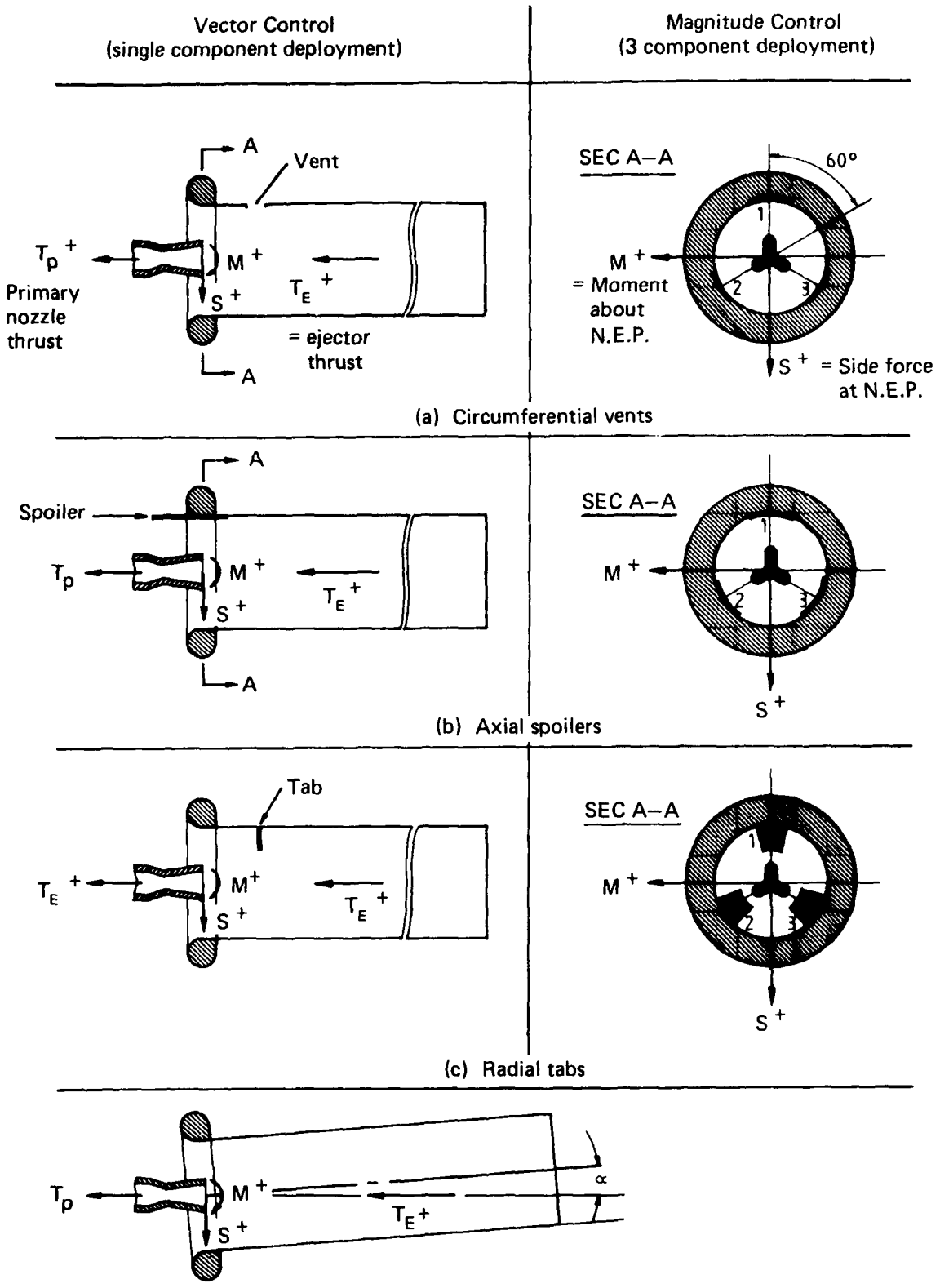

FIG. 5 THRUST CONTROL SYSTEMS WITH 3 LOBE NOZZLE AT 0°

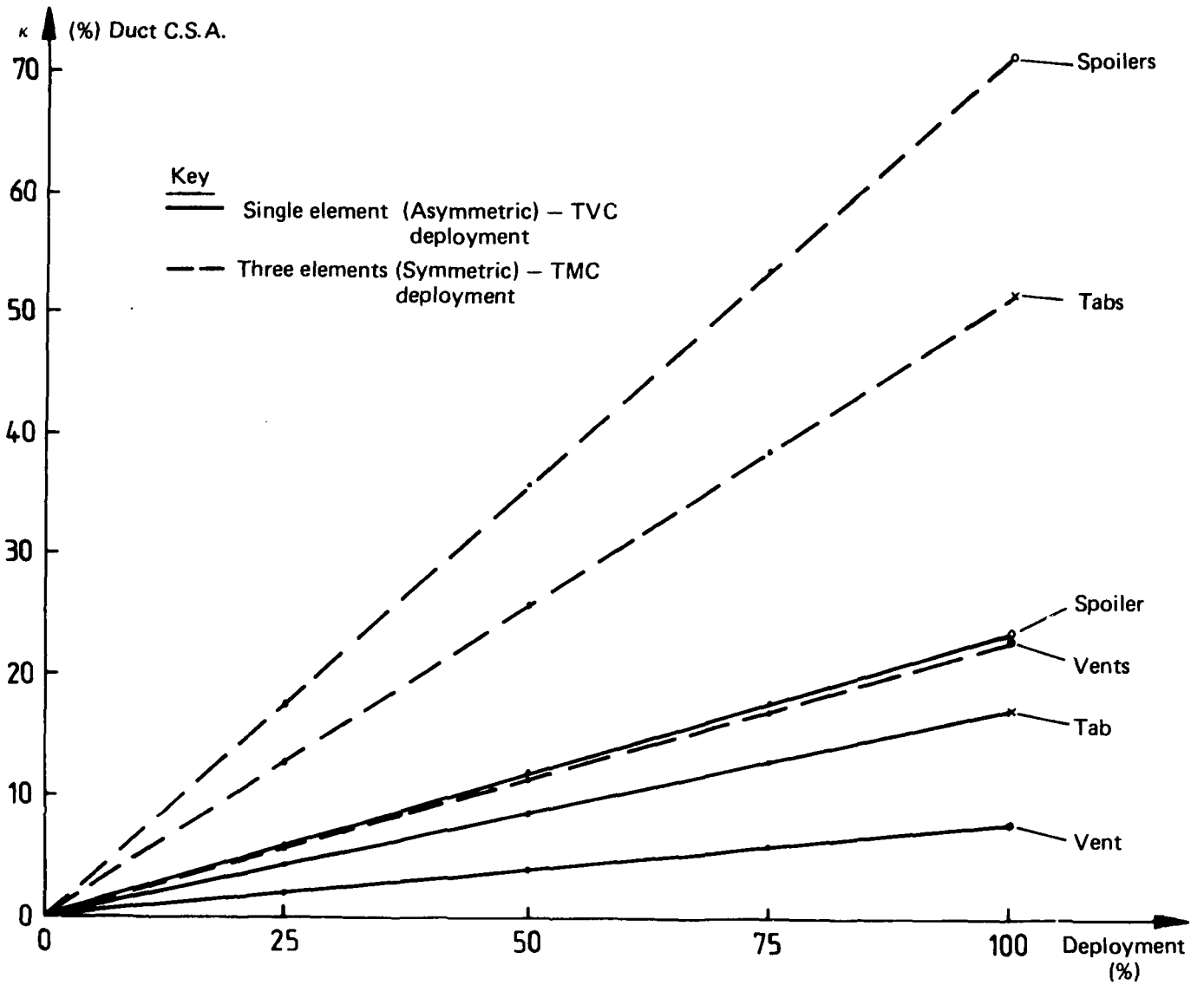

FIG. 6 AREA RATIO, κ vs COMPONENT DEPLOYMENT

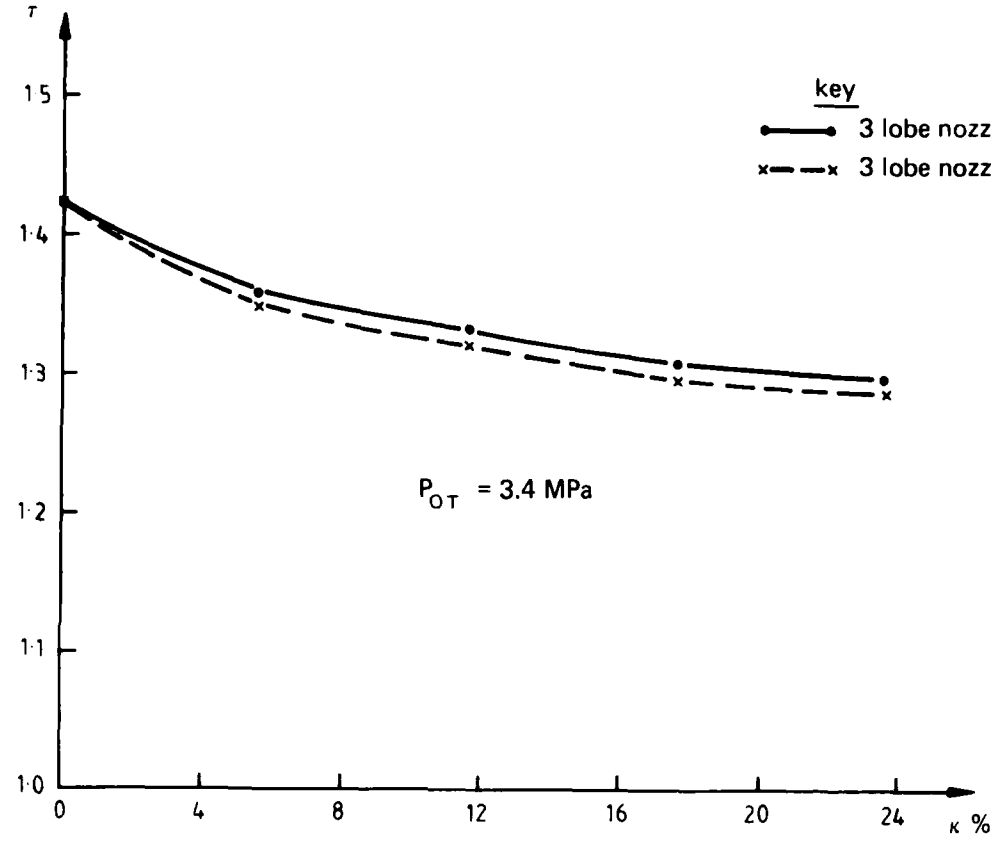

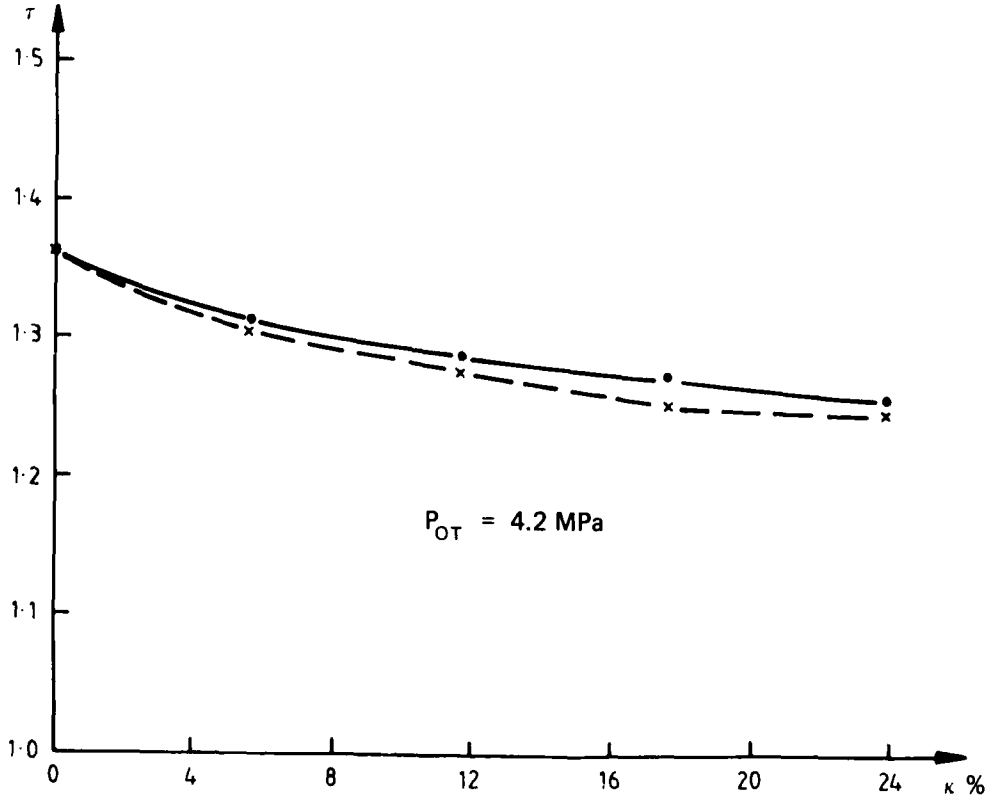

FIG. 7 TMC – CIRCUMFERENTIAL VENTS

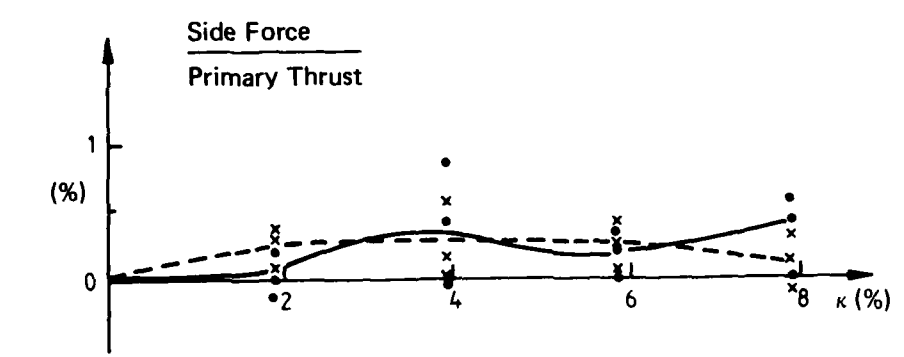

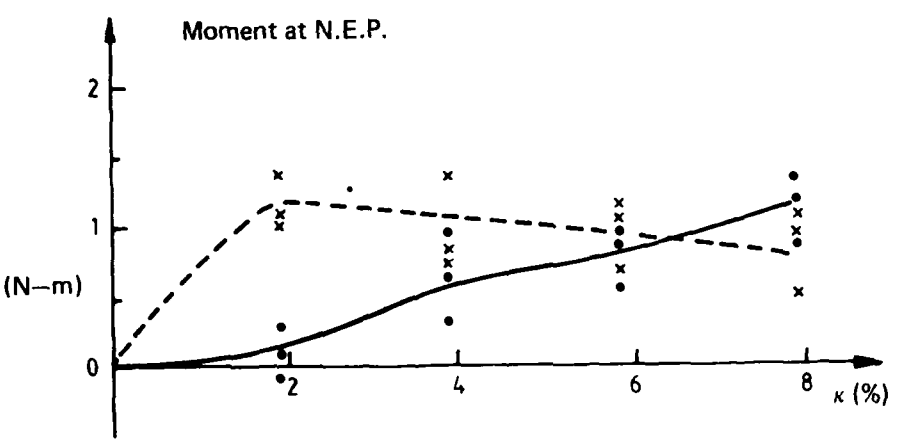

(a) P_{OT} = 34 MPa; Primary Thrust = 310 N

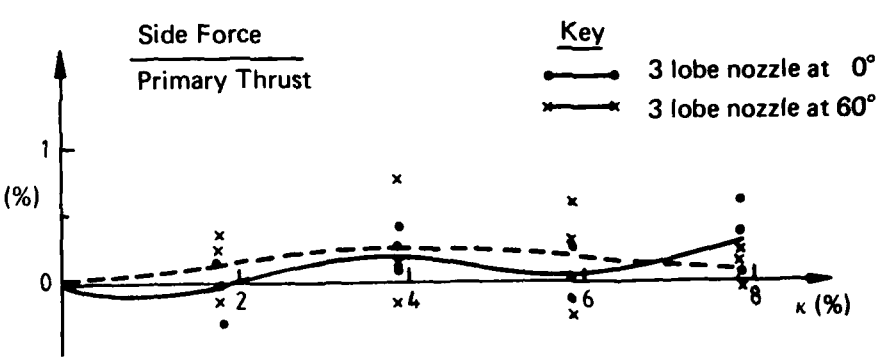

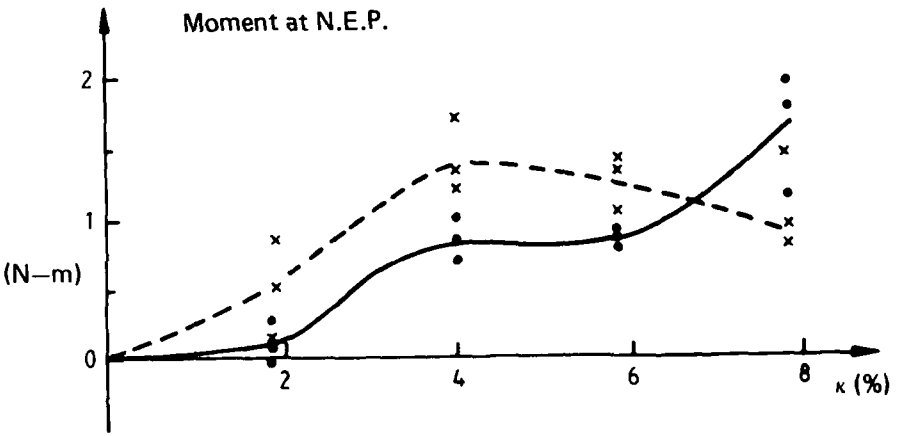

(b) P_{OT} = 4.2 MPa; Primary Thrust = 400 N

FIG. 8 TVC – SINGLE VENT OPENING

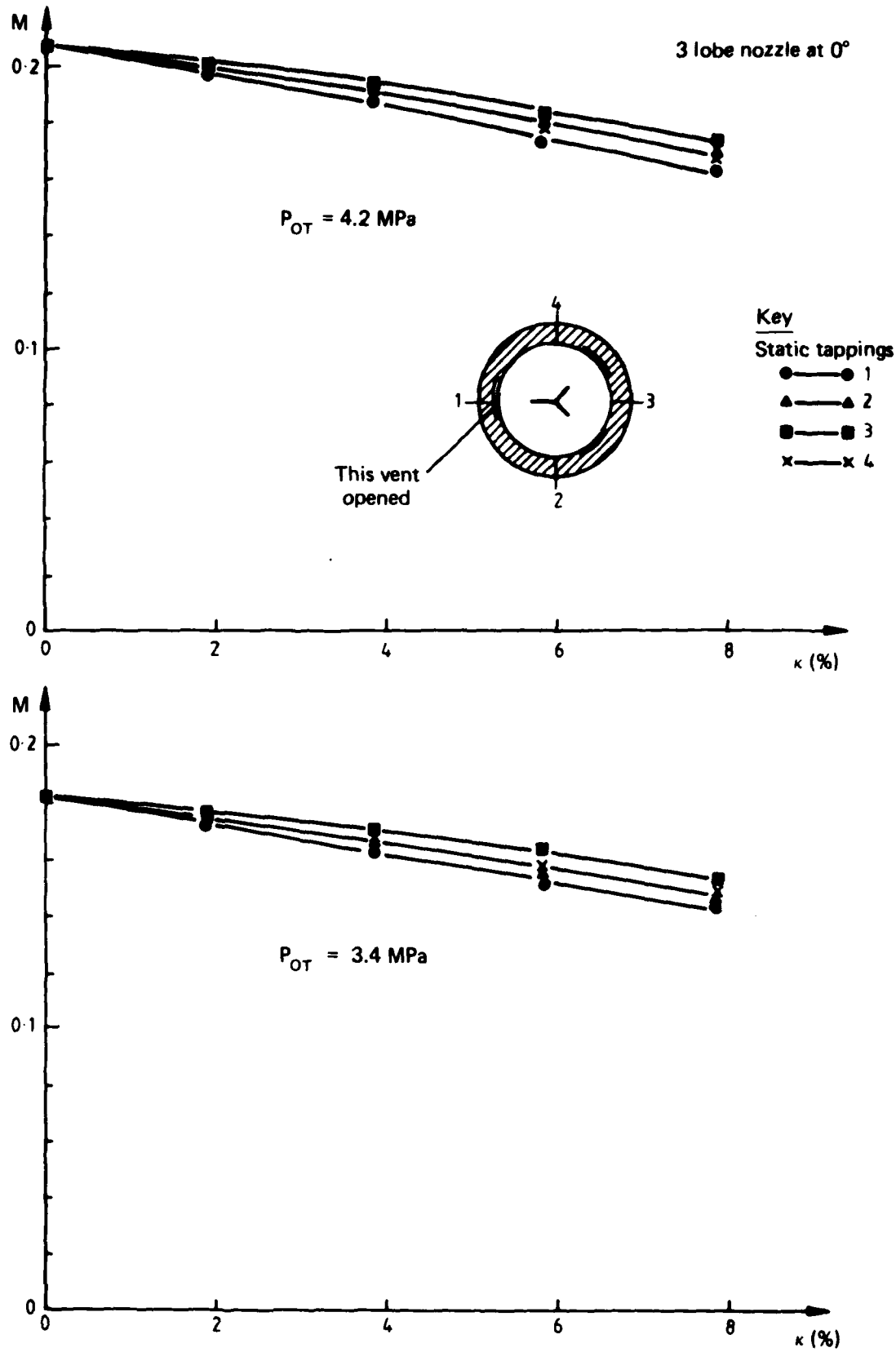

FIG. 9 BELLMOUTH MACH NO. VARIATION vs SINGLE VENT OPENING

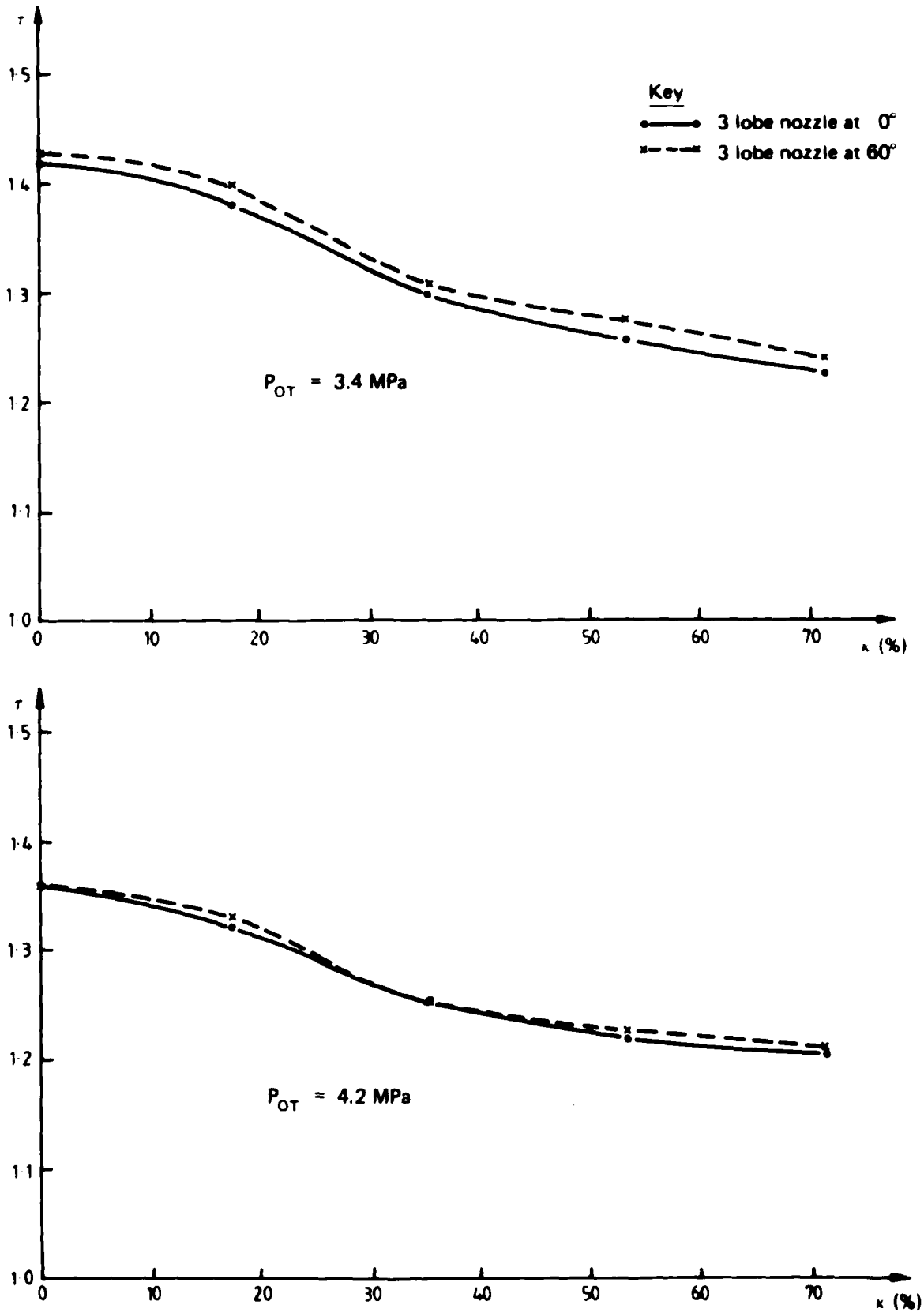

FIG. 10 TMC – AXIAL SPOILERS

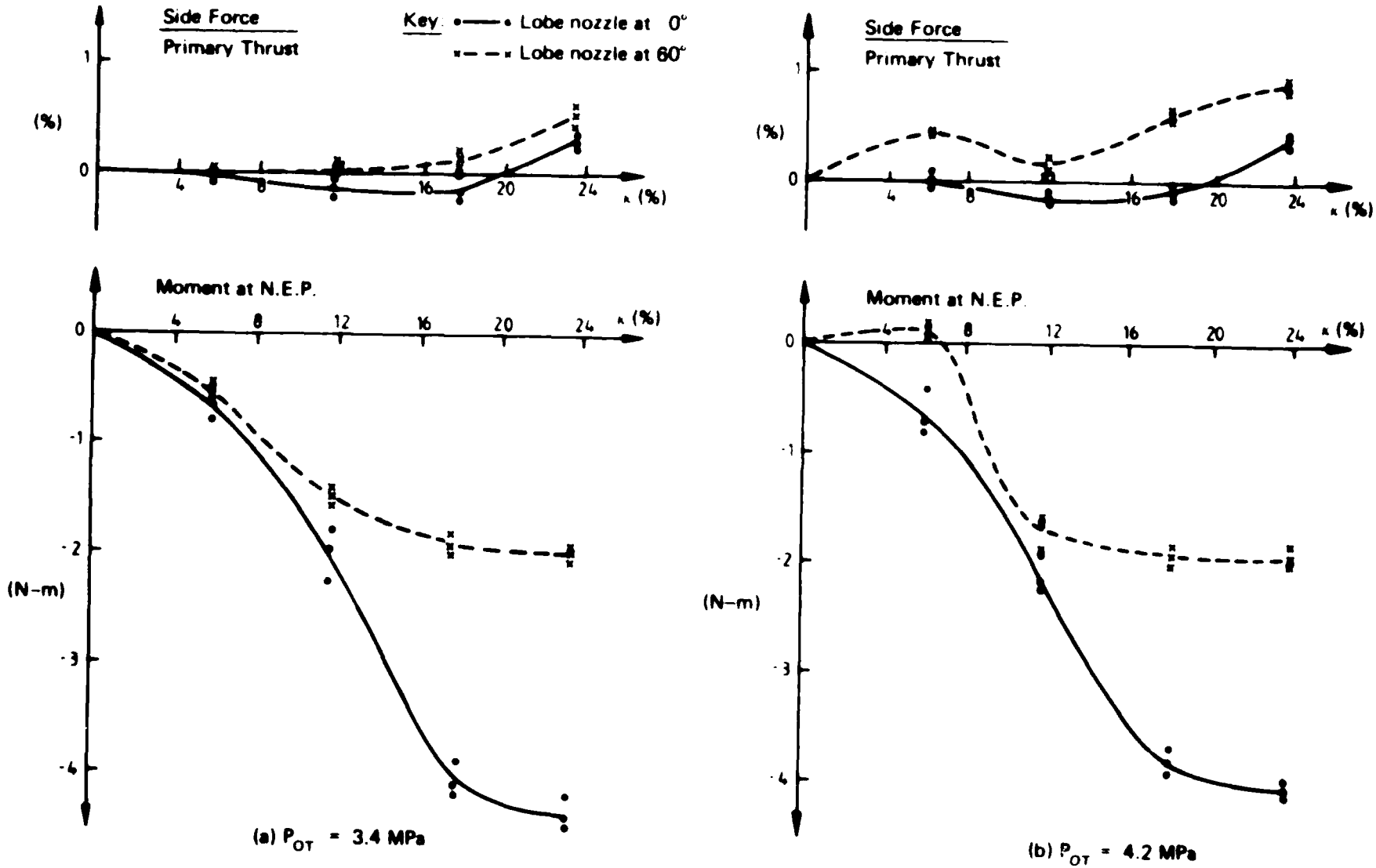

FIG. 11 TVC – SINGLE SPOILER DEPLOYMENT (AXIAL)

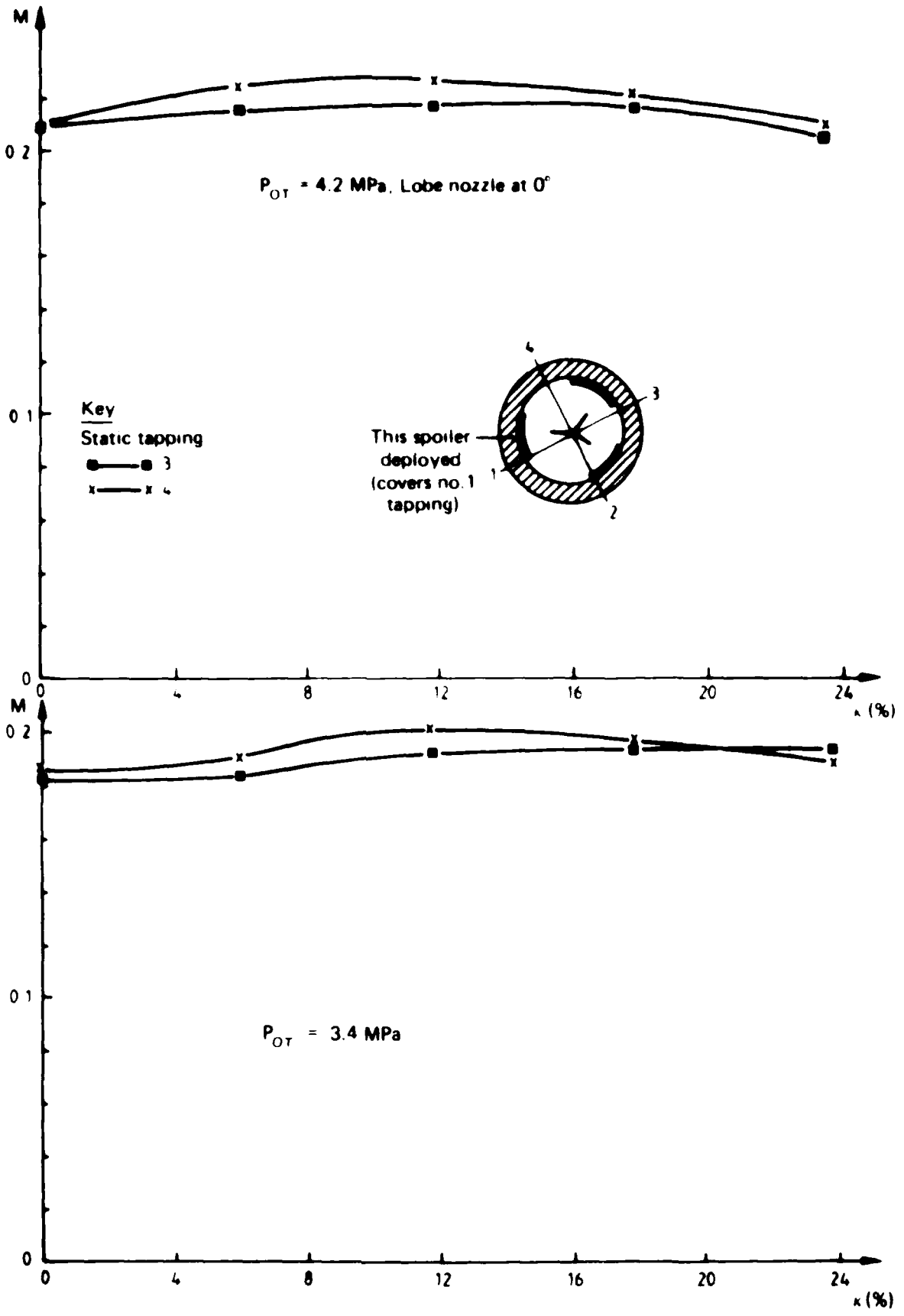

FIG. 12 BELLMOUTH MACH NO. vs SINGLE SPOILER DEPLOYMENT

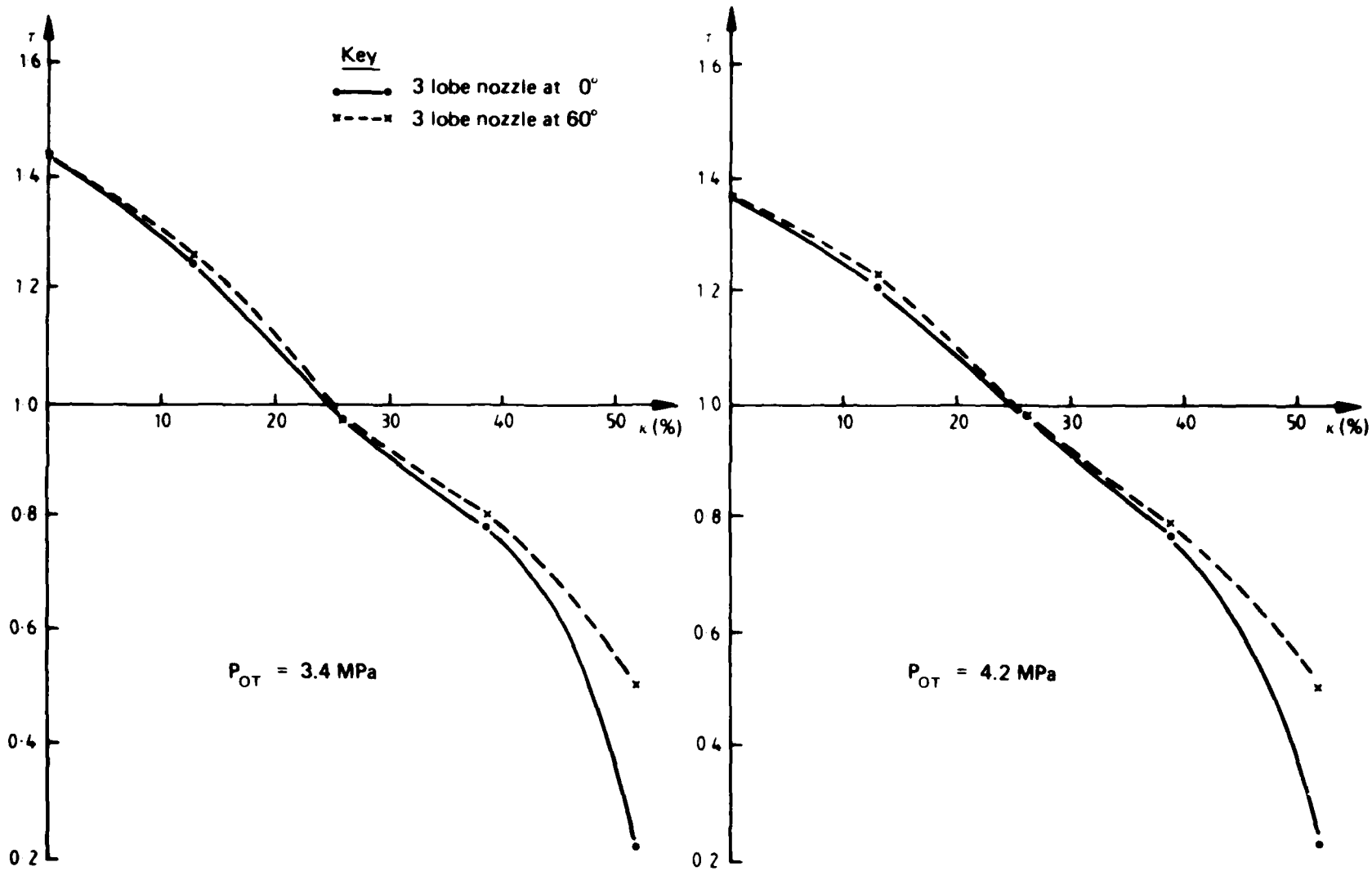

FIG. 13 TMC – RADIAL TABS

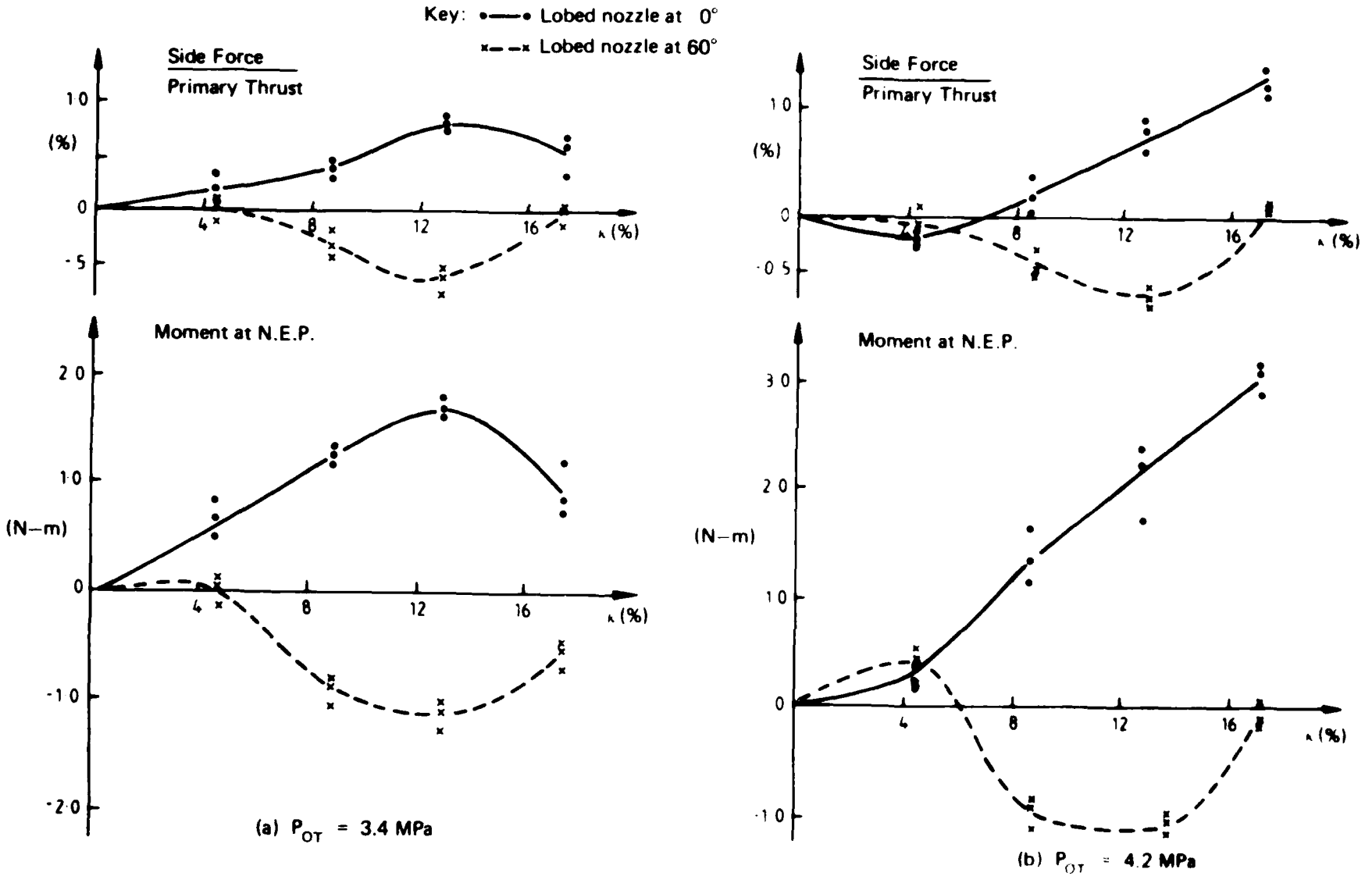

FIG. 14 TVC – SINGLE TAB DEPLOYMENT (RADIAL)

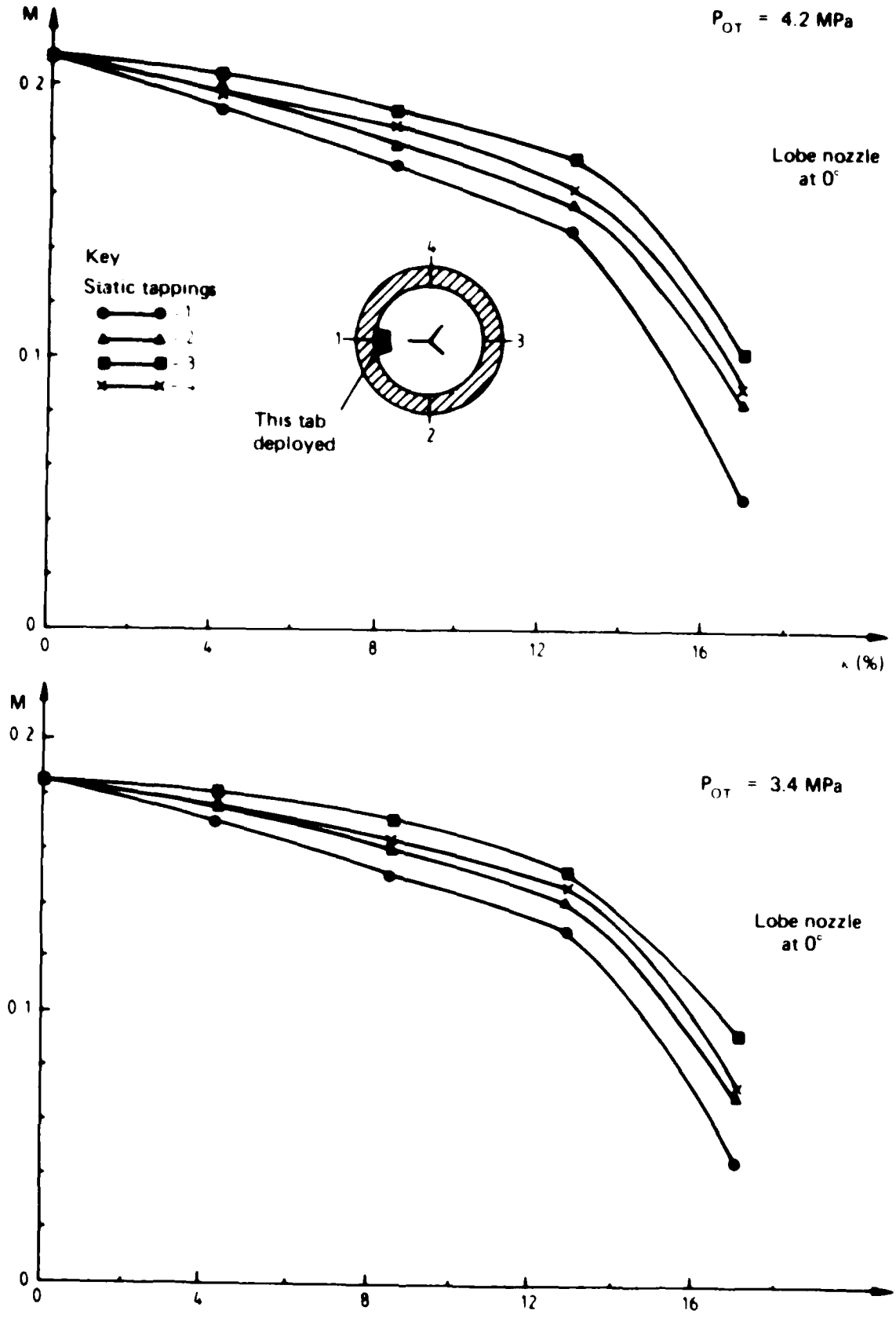

FIG. 15 BELLMOUTH MACH NC vs SINGLE TAB DEPLOYMENT

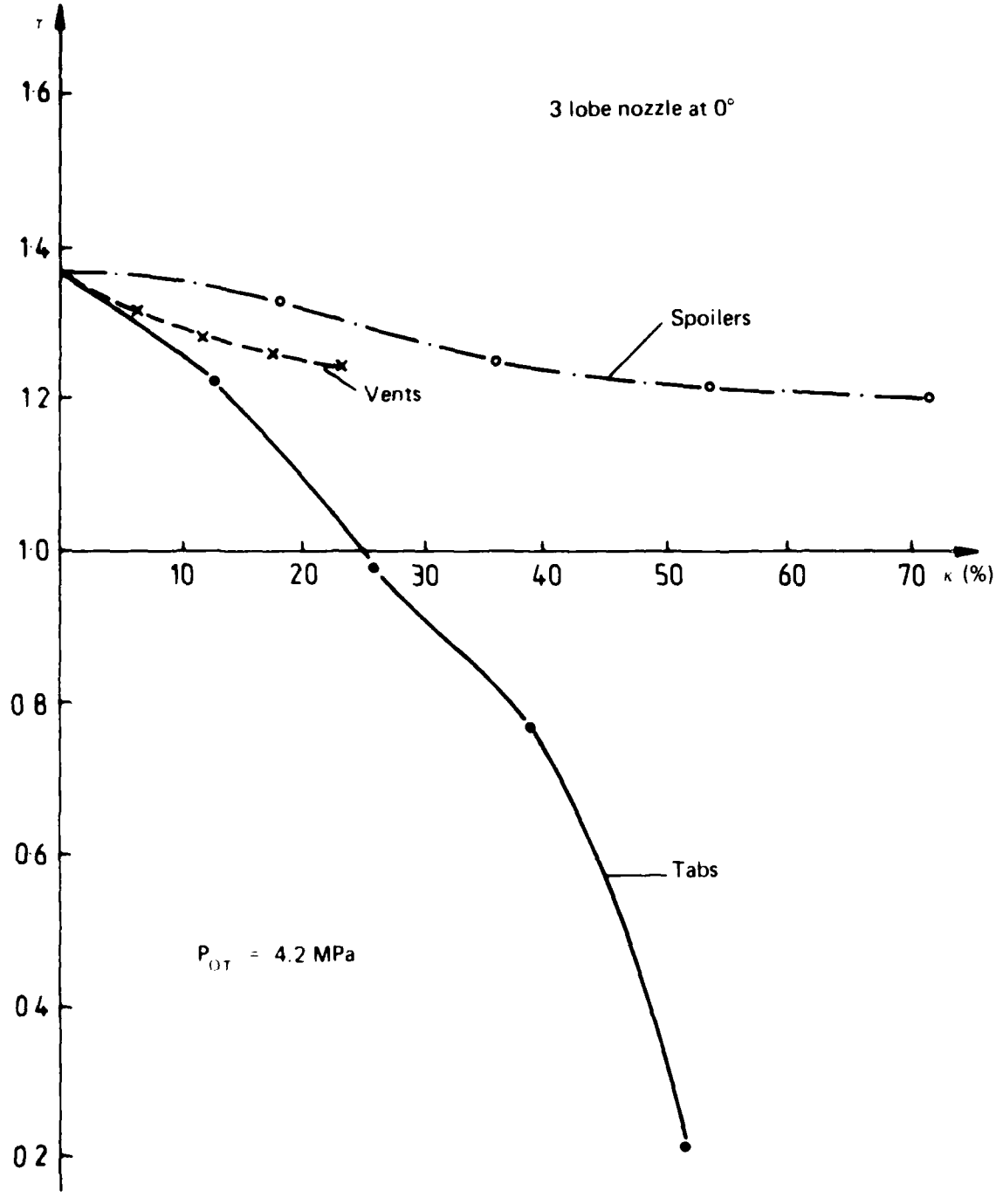

FIG. 16 TMC – COMPARISON

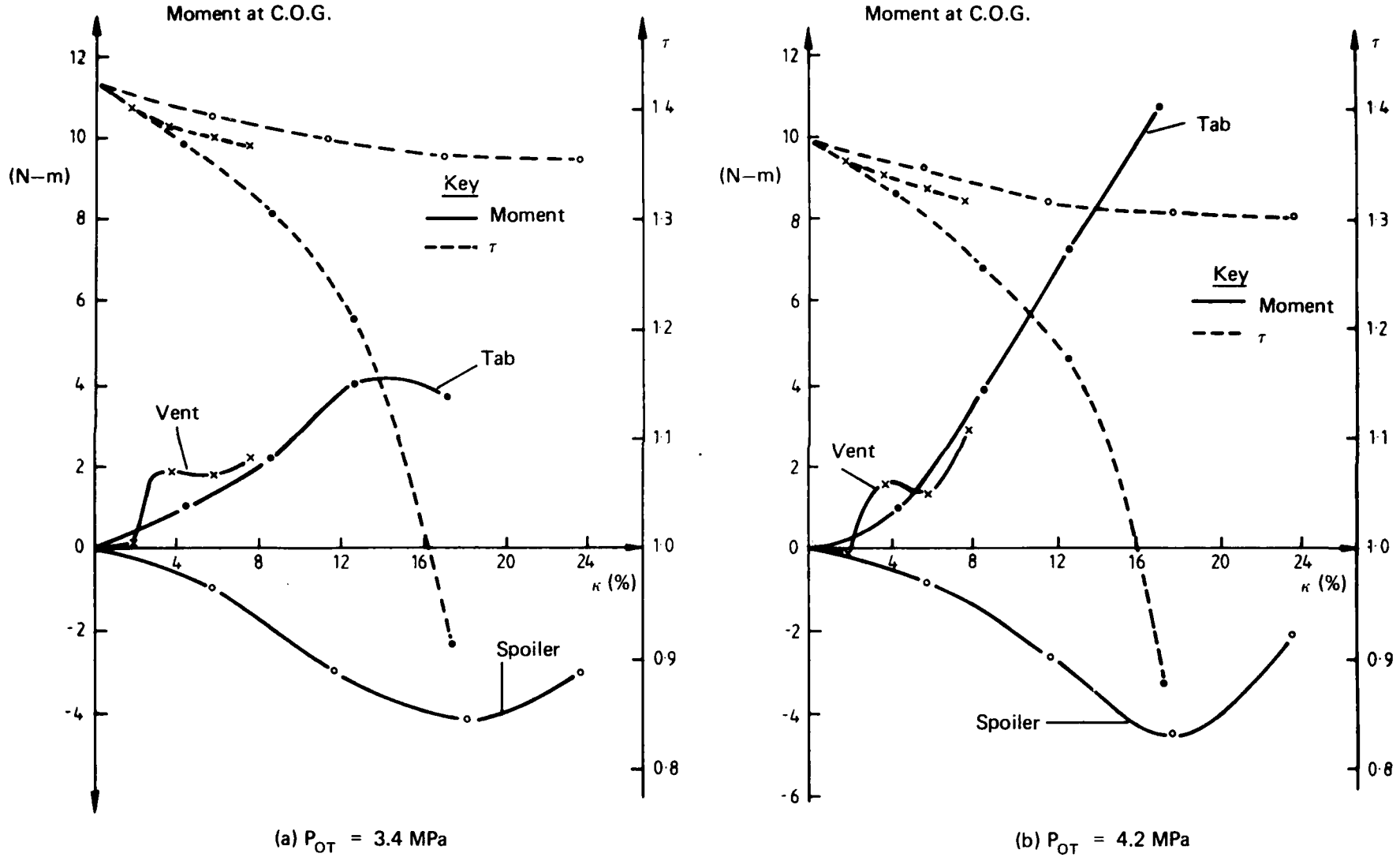

(a) P_{OT} = 3.4 MPa

(b) P_{OT} = 4.2 MPa

FIG. 17 TVC – COMPARISON WITH ASSOCIATED THRUST SPOILAGE – LOBE NOZZLE 0°

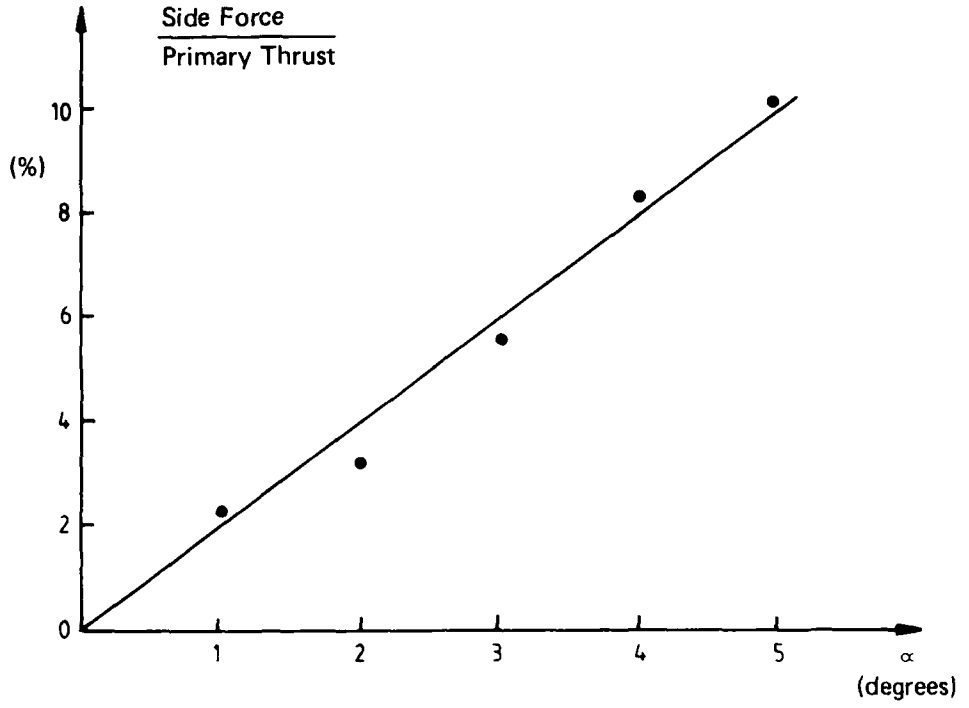

P_{OT} = 4.2 MPa, Lobe nozzle at 0°

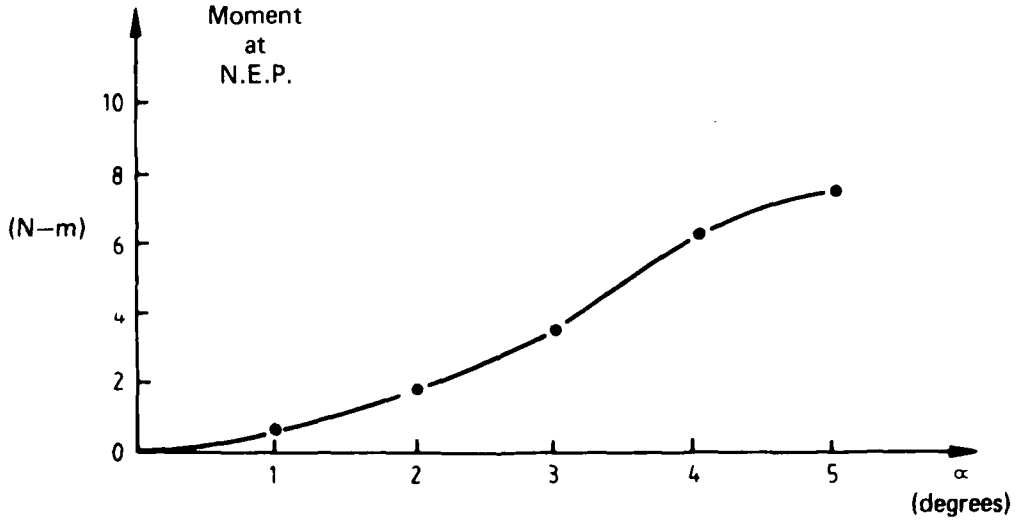

FIG. 18 TVC – DUCT SWIVELLING

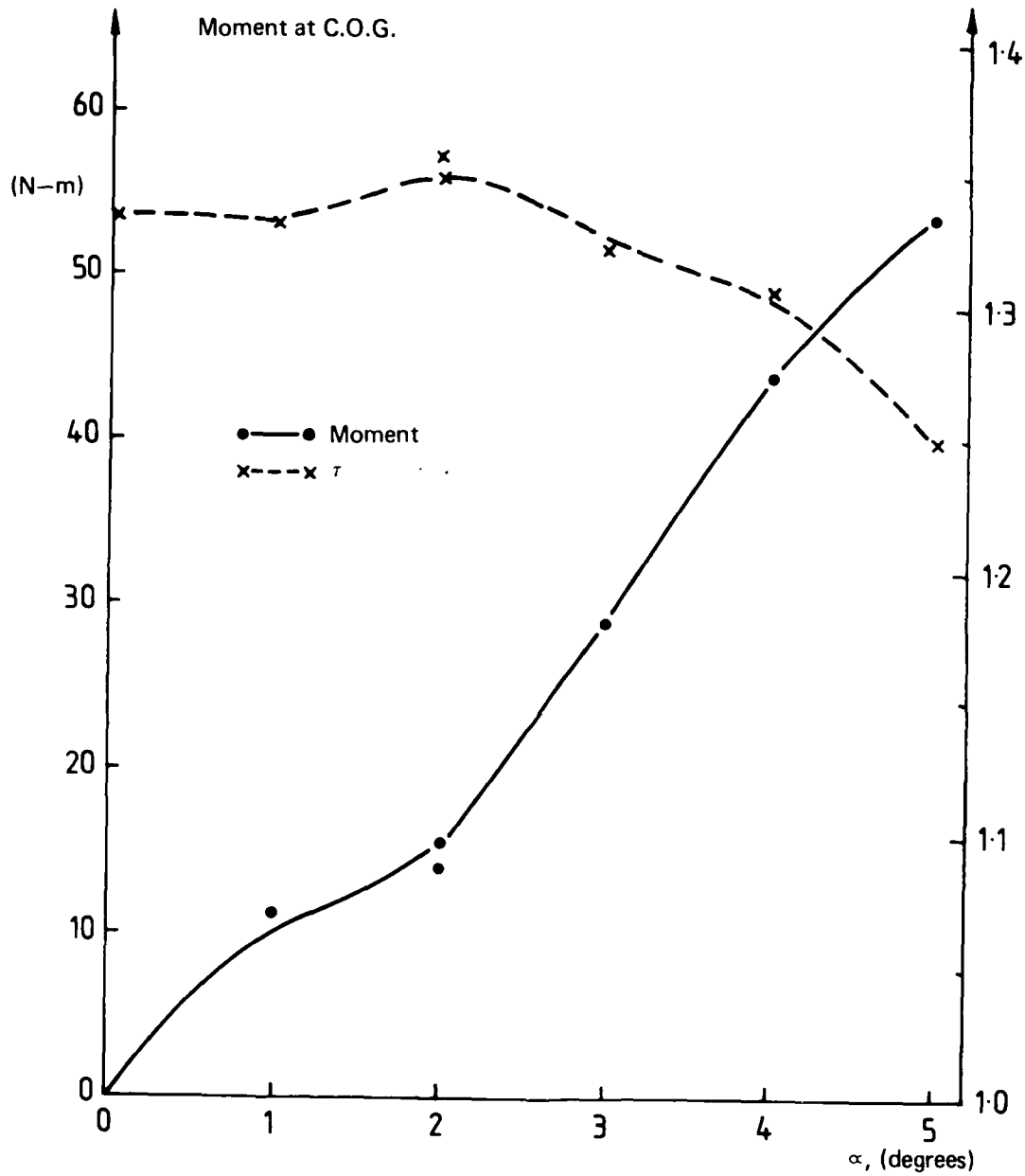

P_{OT} = 4.2 MPa, Lobe nozzle at 0°

FIG. 19 TVC—WITH ASSOCIATED THRUST SPOILAGE — DUCT SWIVELLING

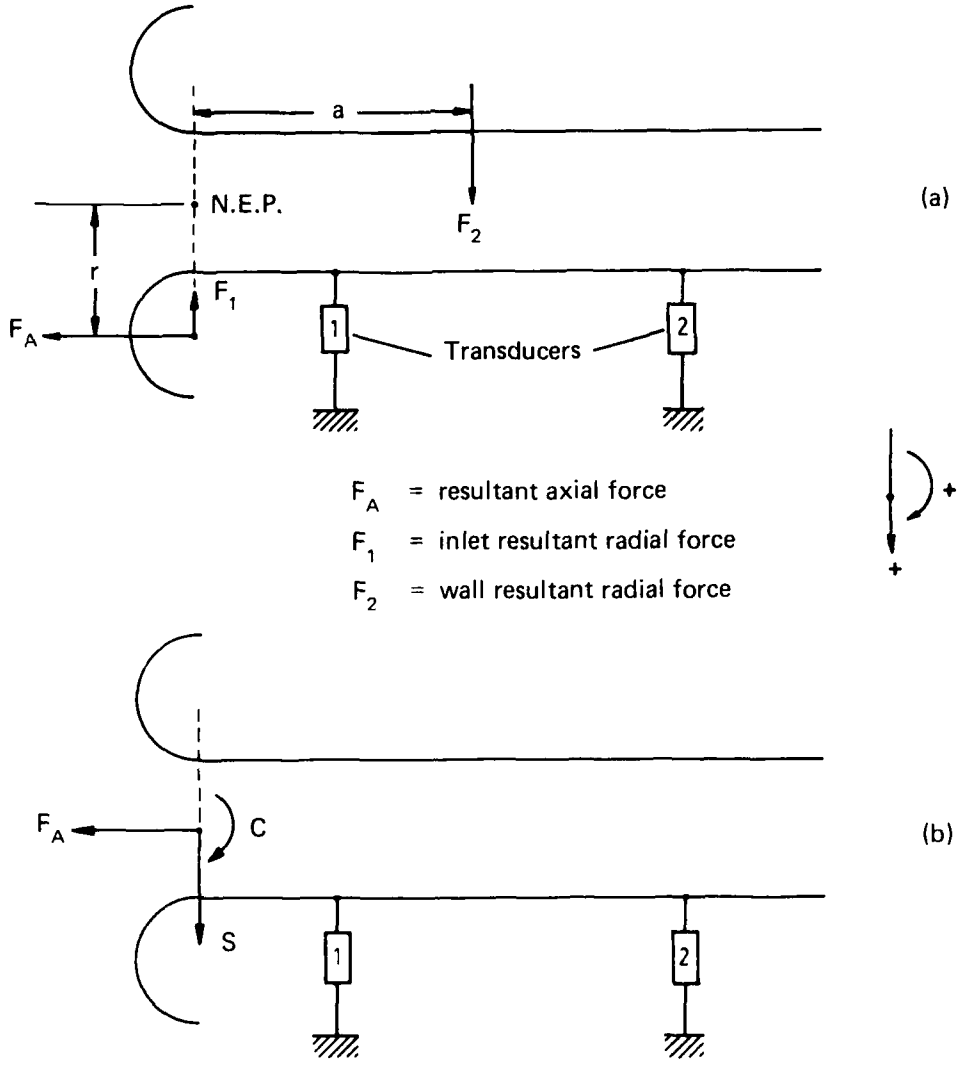

$C = F_2 a + F_A r$

$S = F_2 - F_1$

FIG. A1–FORCE RESOLUTION

DISTRIBUTION

AUSTRALIA

Department of Defence

Defence Central
- Chief Defence Scientist
- Deputy Chief Defence Scientist (shared copy)
- Superintendent, Science and Program Administration (shared copy)
- Controller, External Relations, Projects and Analytical Studies (shared copies)
- Counsellor, Defence Science (London) (Doc Data Sheet Only)
- Counsellor, Defence Science (Washington) (Doc Data Sheet Only)
- Defence Science Representative (Bangkok)
- Defence Central Library
- Document Exchange Centre, DISB (18 copies)
- Joint Intelligence Organisation
- Librarian H Block, Victoria Barracks, Melbourne
- Director General - Army Development (NSO) (4 copies)
- Defence Industry and Material Policy, FAS

Aeronautical Research Laboratories
- Director
- Library
- Superintendent - Aero Propulsion
- Divisional File - Aero Propulsion
- S.A. Fisher
- A.M. Abdel-Fattah
- Author: S C Favaloro

Materials Research Laboratories
- Director/Library

Defence Research Centre
- Library

RAN Research Laboratory
- Library

Navy Office
- Navy Scientific Adviser
- Director, Electronic Warfare - Navy

Army Office
- Scientific Adviser - Army

Air Force Office
- Air Force Scientific Adviser
- Technical Division Library

Central Studies Establishment
- Information Centre

Government Aircraft Factories
Manager
Library

Statutory and State Authorities and Industry
Hawker de Havilland Aust. Pty Ltd, Bankstown, Library
Hawker de Havilland, Victoria, Limited, Library

CANADA
NRC
Aeronautical & Mechanical Engineering Library
Division of Mechanical Engineering, Director

FRANCE
ONERA
Library

JAPAN
National Aerospace Laboratory
Institute of Space and Astronautical Science, Library

NETHERLANDS
National Aerospace Laboratory (NLR), Library

NEW ZEALAND
Defence Scientific Establishment, Library

SWEDEN
Aeronautical Research Institute, Library
Swedish National Defence Research Institute (FOA)

UNITED KINGDOM
Ministry of Defence, Research, Materials and Collaboration
CAARC, Secretary
Royal Aircraft Establishment
Bedford, Library
Pyestock, Director
British Library, Document Supply Centre
Rolls-Royce Ltd, Aero Division Bristol, Library
British Aerospace
Kingston-upon-Thames, Library
Hatfield-Chester Division, Library

UNITED STATES OF AMERICA
NASA Scientific and Technical Information Facility
United Technologies Corporation, Library
Lockheed Missiles and Space Company
McDonnell Aircraft Company, Library

SPARES (10 copies)
TOTAL (79 copies)

Department of Defence

DOCUMENT CONTROL DATA

AD-A183 241

1.a. AR No	1.b. Establishment No	2. Document Date	3. Task No
AR-004-500	ARL-AERO-PROP-R-173	AUGUST 1986	DST82/048

4. Title	5. Security	6. No Pages	7. No Refs
THRUST CONTROL WITH HIGH PRESSURE RATIO EJECTOR AUGMENTORS	a. document: UNCLASSIFIED b. title: U c. abstract: U	40	5

8. Author(s)	9. Downgrading Instructions
S.C. FAVALORO	

10. Corporate Author and Address	11. Authority (as appropriate) a.Sponsor b.Security c.Downgrading d.Approval
Aeronautical Research Laboratories P.O. Box 4331, MELBOURNE, VIC. 3001	

12. Secondary Distribution (of this document)

Approved for public release.

Overseas enquirers outside stated limitations should be referred through ASDIS, Defence Information Services Branch, Department of Defence, Campbell Park, CANBERRA ACT 2601

13.a. This document may be ANNOUNCED in catalogues and awareness services available to ...

No limitations.

13.b. Citation for other purposes (ie casual announcement) may be (select) unrestricted(or) as for 13 a.

14. Descriptions	15. COSATI Group
Thrust vector control Rocket guide vanes Thrust augmentation	21120 01010

16. Abstract

The possibility of utilising the entrained secondary air in a thrust augmenting ejector for thrust control purposes has been examined in a series of experiments using high pressure unheated air as the primary jet.

Four control concepts, namely duct venting, axially deployed spoilers, radially deployed tabs and duct swivelling, have been investigated and results have shown that all systems provide some degree of thrust vector and thrust magnitude control. Maximum TVC in yaw/pitch mode was available with duct swivelling, while radial tabs provided maximum TMC.

PF 65

This paper is to be used to record information which is required by the Establishment for its own use but which will not be added to the DISTIS data base unless specifically requested.

16. Abstract (contd)

17. Imprint

Aeronautical Research Laboratories, Melbourne

18. Document Series and Number	19. Cost Code	20. Type of Report and Period Covered
AERO PROPULSION REPORT 173	423640	

21. Computer Programs Used

22. Establishment File Ref(s)


FILM